TD 91-4194

TNO-report

SAW chemosensor. Third progress report ①

PML 1991-88

AD-A256 487

December 1991
Copy no: -

Author (s):

M.S. Nieuwenhuizen

Total Number of Pages :
(incl. distr. list and RDP)
52

Number of Annexes :
-

Number of Figures :
19

Number of Tables :
13

HDO assignment no.:
A88/K/416

DTIC
ELECTE
S OCT 2 9 1992
A D

Number of Copies :
49

Classification
Report :
UNCLASSIFIED

Title:
UNCLASSIFIED

Summary:
UNCLASSIFIED

Annex(es) :
-

20020225040

92-28394

92 10 28 011

Summary

At the Prins Maurits Laboratory TNO, work on surface acoustic wave (SAW) chemical sensors is being performed. Up to now the main subjects have been: implementation of SAW technology on a silicon chip, the development of a SAW sensor for NO_2 and the development of a SAW sensor for chemical warfare agents.

This third progress report deals with the on-going work on a SAW sensor for NO_2 including immobilization of the chemical interface, silicon-based SAW sensors for NO_2 with and without the application of silicon nitride passivation layers, preliminary results of the development of a SAW sensor for CO_2 and a chapter dealing with an automated SAW testing system developed at TNO-PML. Most of the chapters have been published in the literature.

Samenvatting

Op het Prins Maurits Laboratorium TNO wordt reeds geruime tijd gewerkt aan surface acoustic wave (SAW) chemische sensoren. Tot op heden betrof dit de implementatie van SAW technologie op een silicium chip en de ontwikkeling van een SAW chemische sensor voor NO_2 en voor chemische strijdmiddelen.

Deze derde voortgangsrapportage omvat, in het kader van het werk aan de ontwikkeling van een sensor voor NO_2, de immobilisatie van het chemisch interface en onderzoek aan een SAW NO_2 sensor op silicium, waarbij wel en niet gebruik werd gemaakt van een silicium nitride passiverings-laag. Voorts handelt het rapport over inleidende experimenten aan een SAW sensor voor CO_2 en een beschrijving van het in dit laboratorium ontwikkelde automatische testsysteem. De meeste hoofdstukken zijn gepubliceerd in de literatuur.

Accesion For		
NTIS CRA&I		☒
DTIC TAB		☐
U..announced		☐
Justification		
By		
Dist.ibution /		
Availability Codes		
Dist	Avail a.ıd/or Special	
A-1		

CONTENTS

1   INTRODUCTION

In chemical sensors, chemical signals are transduced into the appropriate electrical signals. These sensors are required to control preset process conditions or are needed for the protection of mankind, fauna and flora by measuring the concentrations of explosive, corrosive or toxic compounds or by warning when pre-selected concentrations are exceeded. A very important link in the automation process is the development of small, robust and inexpensive, yet reliable chemical microsensors.

In contrast to physical signals there is always a variety of chemical signals present at the spot to be monitored. As a consequence, sensor requirements as to selectivity are very important. If one uses a (bio)chemical interface, these requirements can often be met. This interface interacts exclusively with the analyte as selectively as possible, thereby modulating the flow of physical signals in the sensor device.

Sometimes a special (bio)chemical interface is not required as the sensor material acts as a chemical interface; e.g. the metal oxide materials used in semiconductors.

The above-mentioned flow of physical signals is changed to electrical signals by using transducers that convert non-electrical signals into electrical signals. In fact, a (bio)chemical interface is a transducer as well. It transfers signals from the chemical signal domain to the physical or the electrical signal domain.

In recent years, many technologies have been investigated to develop (bio)chemical microsensors [1-3]. Sensors employing electrochemical transduction are most widely studied [4,5]. This category consists of both amperometric and voltammetric sensors. A special example of very small electrochemical sensors is the chemical field effect transistor [6]. In the case of chemiresistors, the resistivity of materials is influenced by the presence of the analyte [7].

Another sensor principle is applied in optical sensors [8,9]. With these sensors, the presence of the analyte brings about a change in optical phenomena. Measurement of light absorption or transmission is often used in combination with waveguides for signal transmission.

As phenomena at the (bio)chemical interface on a microsensor occur in a more or less two-dimensional space, ordinary absorption or transmission techniques are not suitable. Nevertheless, two optical techniques are available at the moment: the evanescent wave technique and surface plasmon resonance.

One of the acoustical sensor principles employs surface acoustic waves (SAW), which has the potential to be applied on a surface rather than in a three-dimensional space. As a result, this technique is very compatible with planar silicon technology, thereby opening possibilities for applying both the sensor and the electronics on a single device: a silicon smart sensor chip [10-12].

The first gas sensor based on a SAW oscillator was reported by Wohltjen and Dessy [13-15] in 1979. The gas sensor consists of a delay-line (one transmitter and one receiver IDT and the free propagation path in between) covered with a polymer [16].
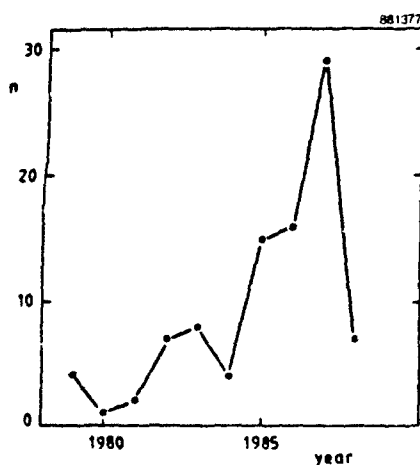
Figure 1   Quantitative development of SAW chemical sensor output after Wohltjen's first paper in 1979

After Wohltjen's first papers, research on SAW chemical sensors exploded as is depicted in Figure 1. Vetelino's group [17,18] reported a SAW dual delay-line structure as a gas sensor. One delay-line is occupied with the (bio)chemical interface and the other, which lies parallel to the first delay-line, acts as a reference.

D'Amico, Palma and Verona [19] reported on a three-transducer-type delay-line (three transducers and two wave paths) again with one free propagation path occupied with the (bio)chemical interface. With these structures, an improved temperature stability was demonstrated.

Where a SAW delay-line sensor employs surface waves travelling between two transducers, a SAW resonator employs standing waves. The sensor shows one or two IDT's which are located between two acoustically reflecting mirrors. The distance between the mirrors allows constructive interference between successive reflections being maximal for one frequency. The first use of a gas sensor based on a SAW resonator was reported by the group of Martin [20-22].

At the Prins Maurits Laboratory TNO, work on SAW chemical sensors was performed in close co-operation with Delft University of Technology, Faculty of Electrical Engineering. Up to now the main subjects have been:

The implementation of SAW technology on a silicon chip, the development of a SAW sensor for NO_2 and the development of a SAW sensor for chemical warfare agents. The results have been published in the open literature [23-33], some patents [34], two progress reports [35,36], one report dealing with biochemical interfaces for chemical warfare agents [37] and three reports dealing with a chemical interface for chemical warfare agents [38-40].

This third progress report deals with the on-going work on a SAW sensor for NO_2 including immobilization of the chemical interface (Chapter 2) [41], silicon-based SAW sensors for NO_2 (Chapters 3, 4 and 5) [42-44], preliminary results of the development of a SAW sensor for CO_2 (Chapter 6) [45] and a paper dealing with the SAW testing system developed at TNO-PML [46]. All chapters have been published previously.

2 A SAW GAS SENSOR FOR NO_2. CHEMICALLY IMMOBILIZED PHTHALOCYANINES AS CHEMICAL INTERFACE

2.1 Introduction

Surface Acoustic Wave (SAW) devices are attractive for chemical microsensor applications because of their small size, low cost, high sensitivity and good reliability. In previous papers [25,29,30,31] we reported on SAW chemical sensor research in our laboratory which was concentrated on the development of a SAW gas sensor for NO_2 using metallo phthalocyanines (applied by sublimation) as so-called chemical interfaces because these compounds show strong interactions with electronegative compounds like NO_2. However, these physically attached chemical interfaces showed drawbacks with respect to response time and stability. Therefore, we introduced the concept of chemical interfaces covalently bonded to the sensor [29,34] using a two-step procedure with a so-called spacer molecule. This spacer molecule (3-aminopropyl triethoxysilane) has at one end a sufficiently reactive group to react with the oxidic detector surface (triethoxysilyl group). At the other end the spacer molecule has an amino group which reacts with the chemical interface molecule (in this case Cu phthalocyanine 4,4',4",4"'-tetracarbonylchloride).

Two main advantages of this spacer concept may be mentioned. Firstly, the reactivity of the surface is enhanced by introducing an amino group which can easily react with carboxylic groups in the phthalocyanine derivative. Secondly, the attainability of the surface is increased by the spacer molecules rising out of the surface.

Although the attainability of such monomolecular interfaces for gases to be measured will be easy (i.e. short response times are to be expected), the sensitivity will be low compared with the thick layers. This problem of reduced sensitivity may be overcome by applying higher frequencies by which higher sensitivities are obtained.

2.2 Results and discussion

In Table 1 the results for NO_2 are listed for both sensor A containing a layer of immobilized tetracarboxy Cu phthalocyanine, and for sensor B on which a 0.45 μm layer of Cu phthalocyanine was applied by sublimation.

Table 1   Sensitivity to NO_2 and response time of 52 MHz SAW gas sensors with an immobilized (A) and sublimated (B) CuPC layer (thickness 0.45 μm) at 70 and 150 °C

T (°C)	Layer	Sensitivity (Hz/ppm)	Response time (min)	Recovery time (min)
70	A	1.5	7	50
70	B	69.1	107	156
150	A	0.3	1	6
150	B	19.8	3	63

It is clear that response times as well as recovery times of sensor A (with the immobilized layer) are smaller both at 70 °C and at 150 °C. At both temperatures it can also be observed that the sensitivity of sensor A is much smaller than that of sensor B, due to the larger amount of adsorptive sites of the sublimated layer on the latter.

In order to use these sensors for automotive applications, however, the response times are still too long. Electron microscopic analysis showed that the spacer does not consist of a monolayer: a layer of polymeric grains is observed. This will affect response times because of diffusion phenomena.

In Table 2 the relative responses (NO_2 = 100) of a number of potentially interfering gases are listed for both sensors at 70 and 150 °C.

Table 2   Relative sensitivities to NO_2 and some other gases of 52 MHz SAW gas sensors with an immobilized layer (A) compared with a sublimated layer (B) at 70 and 150 °C

T (°C)	Layer	Gas:	NO_2	CO_2	CO	CH_4	toluene	NH_3	H_2O	SO_2
70	A		100	0	0	0	0	+145[1]	3	0
70	B		100	0	0	0	0	-1[1]	0.1	0
150	A		100	0	0	0	0	-200[1]	1	0
150	B		100	0	0	0	0	-8[1]	0	0

[1] initial response was taken (partial irreversibility)

It can be concluded that only ammonia and water interfere. The relative response for ammonia of the immobilized layer is very high. This might be due to the polymerization phenomena. The ratio polymeric silane/phthalocyanine is high as a result of this polymerization. Possibly, ammonia strongly interacts with the silane by hydrogen-bridge formation.

The temperature effect on ammonia response is interesting because at 70 °C its sign changes. This, again [25,29,30,31], indicates that SAW responses are not only caused by mass changes but also by conductivity changes and changes in elasticity of the chemical interface layer.

It is to be expected that true monolayers will further improve response times as well as selectivity. Therefore extensive studies to obtain monolayers, using other spacers and/or reaction conditions are in progress, together with the application of higher sensor frequencies.

2.3   Experimental

Reagents. Cu phthalocyanine 4,4',4",4'"-tetracarbonyl-chloride was synthesized according to Shirai et al. [47,48] and its purity was controlled using NMR and IR spectroscopy as well as elemental analysis. All other chemical were obtained commercially and were used without further purification. *Chemical immobilization.* An STX quartz substrate (14x16 mm) containing two identical aluminium delay-lines in a parallel configuration was immersed in fuming nitric acid for 3 min, washed with water several times and dried at room temperature. Subsequently, the substrate was immersed in 100 ml 10% 3-aminopropyl triethoxysilane in toluene and heated at 120 °C for 2 h. After washing with toluene and drying, scanning electron microscopy (SEM) revealed a granular polymeric layer on top of the quartz. Then the substrate was heated at 50 °C for 50 h in 70 ml of chloroform containing 200 mg of Cu phthalocyanine 4,4',4",4'"-tetracarbonyl-chloride and 2 ml of triethylamine. After washing with chloroform and drying, the substrate showed a faint blue colour,

while SEM did not show significant changes in morphology. UV spectroscopy with non-treated quartz as the reference showed two peaks at 213 and 620 nm, while in water (pH = 10) the tetracarboxy Cu phthalocyanine showed three peaks at 219, 326 and 600 nm (p_t = 4.41, 4.17 and 4.18, respectively).

Measurement. The 52 MHz SAW sensors were tested according to the methods and with the equipment described in [30,31].

3 PRELIMINARY RESULTS WITH A SILICON-BASED SURFACE ACOUSTIC WAVE CHEMICAL SENSOR FOR NO$_2$

3.1 Introduction

Surface Acoustic Wave (SAW) devices are attractive for chemical microsensor applications because of their small size, low cost, high sensitivity and good reliability.

For the measurement of the concentration of a specific gas in a mixture of gases, one delay-line of a dual delay-line SAW device must be coated with an appropriate chemical interface, whereas the other delay-line acts as a reference. Physico-chemical interactions occurring at the surface or in the bulk of the chemical interface are responsible for the overall performance characteristics of the gas sensor such as selectivity, sensitivity, reversibility and response time [29].

The physical-electronic system consists of a SAW dual delay-line oscillator implemented in silicon [27]. This requires the application of a piezo-electric zinc oxide (ZnO) layer. In this way, mono-lithic integration of the sensor and the electronic system on a single chip is possible [28].

In previous papers [30,31] a SAW sensor for nitrogen dioxide (NO$_2$) based on piezo-electric STX-cut quartz has been studied intensively. Copper phthalocyanine (CuPC) was preferred as the chemical interface for its selectivity and its response time. In these studies CuPC was applied by Physical Vapour Deposition (PVD). Later on, it was found that chemical immobilization of a CuPC derivative with the help of a spacer molecule, resulting in real chemical bonds between the surface and the chemical interface, is to be preferred because of the increased stability and shorter response time [41].

In this paper, the first results are presented dealing with our studies of the above-described silicon-based SAW sensor with CuPC. The results are compared with the experimental data obtained previously [30,31,41]. It should be noted that during the preparation of this paper, Caliendo et al. [49] also reported on a silicon-based SAW sensor. They used a palladium layer on top of the ZnO-SiO$_2$-Si-layered structure as the chemical interface for the detection of hydrogen.

3.2 Experimental part

The configuration of the silicon- and quartz-based SAW devices and dual delay-line oscillator electronics have been published in detail in [25,27].

The starting material for the fabrication of the sensors was 1-10 Ohm.cm (100) cut Si (300 μm thick) with a thermally grown SiO_2 layer (2 μm thick). The accustic propagation direction on the Si was [001]. ZnO layers (about 20 μm thick) were fabricated by DC sputtering at 7 mTorr using 100% O_2 in a Varian 3119 R&D sputter station. The target to substrate distance was 9 cm and the substrate temperature 400 °C.

CuPC layers were applied by PVD at 10^{-5} Torr in a Balzers Union MED 010 system using a stainless steel mask. The source to substrate distance was 8.5 cm, the source temperature was sufficient for a 0.02 μm/min growth rate.

Layer thicknesses of both ZnO and CuPC layers were determined by Scanning Electron Microscopy. In Figure 2, SEM photographs reveal the layered structure as well as the relative dimensions of the layers.
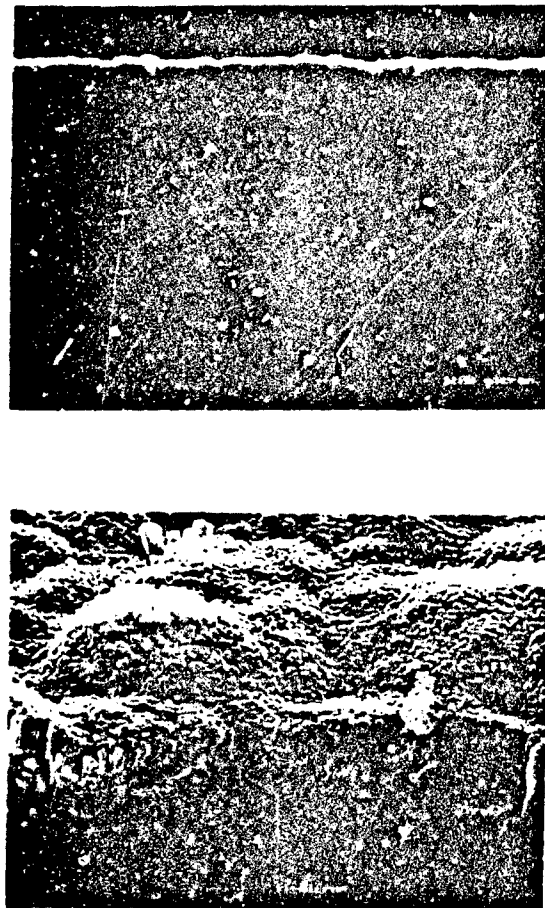
Figure 2   Scanning Electron Micrographs of the silicon - silicon oxide - zinc oxide -
Cu phthalocyanine layered structure.
Top: full picture. Bottom: detail of top layer

The electronic system consisted of two insulated identical oscillators. The output signals of both delay-lines were measured separately and the difference calculated by a computer.

In Table 3 the different sensors tested are listed as well as their frequency, layer thickness of CuPC, medium-term drift and peak-to-peak noise. The silicon-based system was coated with CuPC using PVD. Two configurations nave been investigated; a layer was applied both on the wavepath in between the emitting and receiving transducer of one delay-line (sensor code: CuPC134) or on the delay-line as a whole (sensor code: CuPC135). With the quartz sensors, CuPC was applied in the same way in between the transducers (sensor code:CuPC65) or on the delay-line as a whole (sensor code: CuPC76) Also quartz with a chemically immobilized CuPC layer has been studied (sensor code: CuPCI87).

Table 3   Description of different sensor types in which mask = PVD in between transducers, all = PVD on the whole delay-line, CI = chemically immobilized CuPC, h = thickness of PC-layer, D = drift and N = peak-to-peak noise

Code	Type	Frequency (MHz)	PC layer	h (µm)	D (Hz/min)	N (Hz)
CuPC134	$ZnO\text{-}SiO_2\text{-}Si$	70	mask	1.1	-2.1	110
CuPC135	$ZnO\text{-}SiO_2\text{-}Si$	70	all	1.0	-71.0	200
ZnO	$ZnO\text{-}SiO_2\text{-}Si$	70	-	-	-9.2	180
CuPC65	quartz	52	mask	0.45	0.8	7
CuPC76	quartz	80	all	0.40	-0.3	22
CuPC187	quartz	52	CI	-	-1.9	10
quartz	quartz	80	-	-	-1.4	40

In Figure 3, schematic views of the different sensor configurations studied are shown.

A description of the experimental test system and definitions of response, response time and sensitivity have been published previously [30,31].

890127

CuPC 65

CuPC 76

CuPCI 87

CuPC 134

CuPC 135
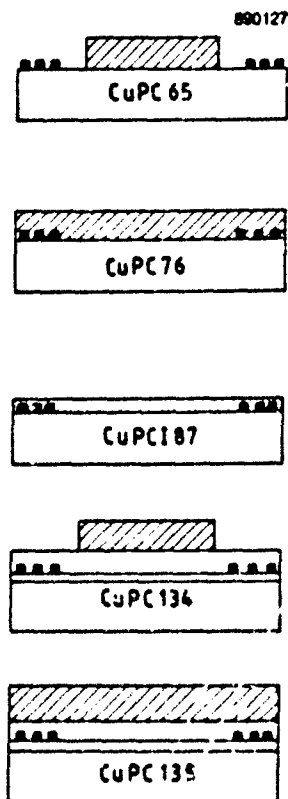
Figure 3   Schematic pictures of the different sensors studied. Sensor codes refer to details given
in Table 3

3.3   Results and discussion

In Table 4, the responses are shown for the sensors described in Table 3. In the table, previous
results with the quartz-based system are also presented. For the sake of reference here also the
responses of the reference ZnO and quartz delay-lines are given.

The sensitivity of a SAW sensor is related to the frequency of the device. This implies that the
results given cannot be easily compared. In Table 4, calculated results are included normalized at a
frequency of 70 MHz using a relationship between the sensitivity and frequency squared.

Table 4   Sensitivity (S) and sensitivity normalized to 70 MHz (between brackets) and 80 % response times (RT) of the different sensor types for NO_2, NH_3 and H_2O at 150 °C. The $ZnO-SiO_2-Si$ results are single delay-line measurements

Code	Frequency	NO_2			NH_3		H_2O
		S		RT	S		s
	(MHz)	(Hz/ppm)		(min)	(Hz/ppm)		(Hz/ppm)
CuPC134[1]	70	200.0		10	-1.0		0.0
CuPC135[1]	70	920.0		7	-5.2		0.0
ZnO[1]	70	40.0		10	-0.7		-0.1
CuPC65	52	19.8	(35.1)	3	-1.6	(-2.9)	0.0
CuPC76	80	-74.0	(-56.7)	7	3.7	(2.8)	0.0
CuPC187	52	0.3	(0.5)	1	-0.6	(-1.1)	0.003
quartz[1]	80	0.0		-	0.0		0.0

[1] single delay-line measurements

With the quartz sensors, two points of interest were noticed. The response time of the sensor with the immobilized layer proved to be shorter due to less diffusion of NO_2 into the monolayer. Moreover the sensitivity of this sensor was much smaller than that of the other sensors. This is most probably due to the smaller amount of adsorptive sites.

Surprisingly, in the quartz system application of a CuPC layer on the delay-line as a whole caused a change in the sign of the response as well as an increased absolute value. Work is in progress to find an explanation for this behaviour.

All experiments carried out with the silicon-based sensors were performed with the occupied single delay-line instead of a dual delay-line configuration. This was done because the reference delay-line also showed a response for NO_2, which is partly irreversible with an initial response of 40 Hz/ppm. This ZnO reference delay-line also responded with a negative sign to the presence of water or ammonia. These observations are in contrast with the work of Martin et al. [21] concerning water adsorption at 24 °C by a 109 MHz silicon-based resonator. The results of the silicon-based sensors can easily be compared with quartz dual delay-line results as the quartz reference delay-line does not respond at all to the gases tested.

As bare ZnO is not able to play the role as reference delay-line in forthcoming experiments, the ZnO has to be coated with a passivation layer in order to prevent the interaction between ZnO and the analytes or interferences. Work is in progress to find a suitable passivation layer. Vellekoop et al. [50] have already reported on previous results.

In Table 4, the results are listed for both CuPC in between the transducers and all over the sensor. It is shown that the sign of the response of the latter sensor is positive in contrast with that of a similar quartz sensor. This is possibly due to the fact that in the quartz system CuPC contacts the aluminium transducers which is not the case in the silicon-based system. At the moment there is no clear picture of the background of the phenomena observed. Work, both theoretical and experimental, is in progress in order to get a better insight.

It has also been observed that the sensitivity of the silicon-based sensor is larger than the quartz-based sensor even when compensated for differences in layer thickness and frequency. These results are in accordance with the work of Caliendo et al. [49]. They studied a palladium layer for the detection of hydrogen on $ZnO-SiO_2-Si$, quartz and lithium niobate.

Figure 4 shows the response of sensor CuPC134 versus the NO_2 concentration in the 20-100 ppm range. The curve shows the same saturation behaviour as the curves for the quartz-based sensors presented previously [30], which indicates that similar physico-chemical processes play a role.

In Table 4, responses for the interferences ammonia and water are also listed. In previous studies [30,31,41], these gases proved to show some response at 150 °C. With the immobilized CuPC layer on the quartz sensor, an extremely strong interference of ammonia was observed. This is probably due to interaction with the spacer (3-aminopropyl triethoxy silane), which partly polymerizes [41].

Furthermore, it was noticed that both the silicon- and quartz-based sensors with CuPC show a negative response for ammonia along with a partly irreversible and fatiguing effect.
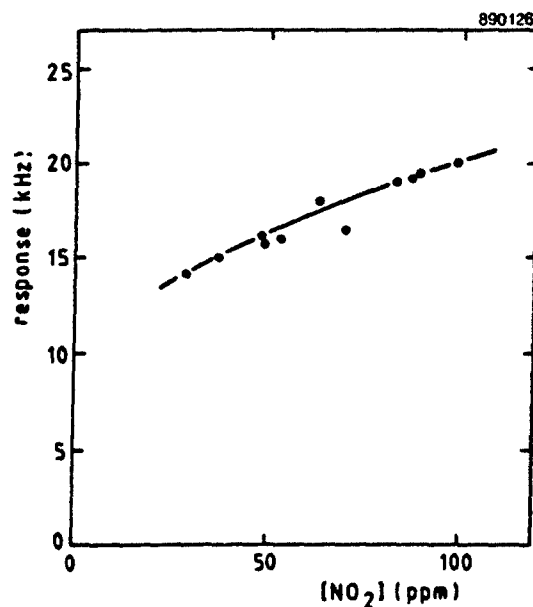
Figure 4   Response of the silicon-based sensor CuPC134 as a function of the NO_2 concentration at 150 °C

It can be clearly observed that response times, as well as recovery times, of sensor A (with the immobilized layer) are smaller both at 70 °C and at 150 °C. At both temperatures it can also be seen that the sensitivity of sensor A is much smaller than that of sensor B, due to the larger amount of adsorptive sites of the sublimated layer on the latter.

In order to use these sensors for automotive applications, however, the response times are still too long. Electron microscopic analysis showed that the spacer does not consist of a monolayer: a layer of polymeric grains is observed. This will affect response times because of diffusion phenomena.

In Table 5, the relative responses (NO_2 = 100) of a number of potentially interfering gases are listed for both sensors at 70 and 150 °C.

Table 5   Relative sensitivities to NO_2 and some other gases of 52 MHz SAW gas sensors with an immobilized layer (A) compared with a sublimated layer (B) at 70 and 150 °C

T (°C)	Layer	Gas:	NO_2	CO_2	CO	CH_4	toluene	NH_3	H_2O	SO_2
70	A		100	0	0	0	0	+145[1]	3	0
70	B		100	0	0	0	0	-1[1]	0.1	0
150	A		100	0	0	0	0	-200[1]	1	0
150	B		100	0	0	0	0	-8[1]	0	0

[1] initial response was taken (partial irreversibility)

It can be concluded that only ammonia and water interfere. The relative response of the immobilized layer for ammonia is very high. This might be due to the polymerization phenomena. The ratio polymeric silane/phthalocyanine is high as a result of this polymerization. Possibly, ammonia strongly interacts with the silane by hydrogen-bridge formation.

The temperature effect on ammonia response is interesting because at 70 °C its sign changes. This, again [25, 29, 30, 31] indicates that SAW responses are not only caused by mass changes but also by conductivity changes and changes in elasticity of the chemical interface layer.

It is to be expected that true monolayers will further improve response times as well as selectivity. Therefore extensive studies to obtain monolayers using other spacers and/or reaction conditions are in progress, together with the application of higher sensor frequencies.

3.4   Conclusions

Preliminary results show the feasibility of a silicon-based SAW sensor system with a ZnO-SiO_2-Si-layered structure as a chemical sensor. The sensitivity of an NO_2 sensor of this type using Cu phthalocyanine as the chemical interface is much higher than the quartz-based system.

Dual delay-line measurements with the silicon-based sensors to improve temperature stability and other common mode effects can only be performed when a passivation layer has been applied, as ZnO interacts with all kinds of gases to give considerable responses of the reference delay-lines.

4 A SILICON-BASED SAW NO$_2$ SENSOR USING A SILICON NITRIDE PASSIVATION LAYER

4.1 Introduction

Surface Acoustic Waves (SAW) devices are attractive for many gas sensor applications [10]. The response mechanism is a combination of the effect of changes of mass, conductivity and elasticity of a thin coating applied on the SAW device: the chemical interface.

In a previous paper [42] we reported on an Si-SiO$_2$-ZnO-layered dual delay-line SAW sensor for NO$_2$ employing copper phthalocyanine (CuPC) as the chemical interface. The (non-occupied) reference delay-line of this sensor showed undesirable responses to various gases due to their interaction with the ZnO.

Upon the application of a silicon nitride passivation layer on top of the ZnO, a positive effect on the reference delay-line (smaller responses by a factor 1.3 to 130) was found [51].

The present paper describes the effect of silicon nitride passivation on the properties of the Si-SiO$_2$-ZnO-layered device as a sensor for NO$_2$. More detailed description of the work will be presented in [44].

4.2 Experimental part

Detailed information on the production of the silicon-based sensors with silicon nitride layers [42,44,51] and CuPC layers, as well as on the experimental test system [30,] can be found in the literature.

In Table 6, the CuPC layer thickness, frequency, medium-term drift and peak-to-peak noise of both sensors are listed. The passivated sensors showed less drift but noise levels were comparable.

Furthermore the sensitivity to NO$_2$ (normalized to the CuPC thickness) and the relative sensitivity of both sensors to NH$_3$ and H$_2$O at 30 °C and 150 °C are listed in Table 6. In the case of H$_2$O, very high concentrations had to be applied in order to obtain measurable responses.

Table 6   Sensitivity to NO_2 (normalized to the CuPC thickness) and relative sensitivity of both sensors to NH_3 and H_2O at 30 °C and 150 °C

		Si-SiO$_2$-ZnO-CuPC		Si-SiO$_2$-ZnO-nitride-CuPC	
Thickness CuPC	(μm)	1.0		0.5	
Temperature	(°C)	30	150	30	150
Frequency	(MHz)	70.20	70.71	72.41	72.23
Drift	(Hz/min)	0.6	8.5	0.5	1.5
Noise	(Hz)	20	110	20	70
S NO_2	(Hz/ppm.μm)[1]	92	124	240[2]	16
S NH_3/S NO_2	(%)	-10	-4	0.2	-9
S H_2O/S NO_2	(%)	-0.12	-0.02	-0.06	-0.13

[1] S = sensitivity

[2] very slow response and independent of concentration

4.3   Results and discussion

With respect to the *sensitivity* to NO_2, the passivated sensor showed peculiar behaviour at 30 °C. The response became slow and independent of the NO_2 concentration. No explanation can be given for this phenomenon.

In the case of the passivated sensor, the conductivity effect on the response can be neglected as a result of the presence of the silicon nitride layer. Therefore the sensitivity to NO_2 at elevated temperatures decreases due to decreasing adsorption of NO_2 (mass effect).

Without a silicon nitride layer the conductivity effect cannot be neglected any longer. The effect of temperature on the sensitivity to NO_2 is due to a combination of the effect of temperature on conductivity changes and on mass changes. The former effect probably dominates resulting in a higher sensitivity at elevated temperatures. At 150 °C, passivation yielded a lower sensitivity to NO_2 (Figure 5).

Upon passivation, *selectivity* with respect to ammonia and water is negatively affected at 150 °C (Table 6). As a result of the different response mechanisms already mentioned above, the relative sensitivity to ammonia and water differs for the two sensors and the two temperatures. The effect of penetration of small molecules through the silicon nitride layer cannot be totally excluded.

At 150 °C, non-passivated delay-lines are preferable to passivated delay-lines with respect to both sensitivity and selectivity to NO_2.
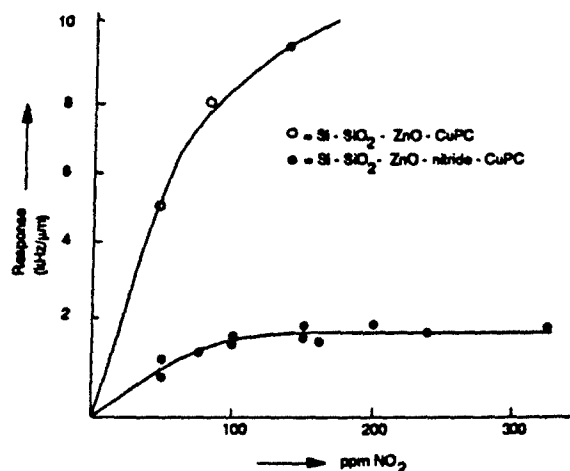
Figure 5   Response curves for NO_2 of both a passivated and a non-passivated sensor

4.4   Conclusions

Silicon nitride has been applied as a passivation layer to prevent gases from interacting with the ZnO of the Si-SiO$_2$-ZnO SAW sensor system. On such a sensor, conductivity changes hardly affect SAW responses.

Sensitivity to NO_2 decreases as a result of passivation while selectivity with respect to water and ammonia becomes worse.

A good compromise between these results may be a sensor with a passivated reference delay-line and a measuring delay-line completely covered with the chemical interface. Work is in progress to study this compromise.

5 A SILICON-BASED SAW CHEMICAL SENSOR FOR NO_2 BY APPLYING A SILICON NITRIDE PASSIVATION LAYER

5.1 Introduction

Surface Acoustic Waves (SAW) devices are attractive for chemical gas sensor applications because of their small size, low cost, high sensitivity and good reliability [10,12]. To measure the concentration of a specific gas in a mixture, the measuring delay-line of a dual delay-line SAW device must be coated with an appropriate chemical interface. The other delay-line acts as a reference.

In previous papers [25-27,29-31,41] we reported on a quartz-based SAW sensor for NO_2 employing metallo phthalocyanines, mostly copper phthalocyanine (CuPC), as the chemical interface. After the introduction of silicon-based SAW sensors by other groups [21,52] we also introduced [42] a physical-electronic system consisting of a dual delay-line oscillator implemented in silicon. This required the application of a piezo-electric zinc oxide (ZnO) layer. In this way, monolithic integration of the sensor and the electronics on a single silicon chip was possible.

The first experimental results dealing with silicon-based SAW chemical sensors were presented employing the Si-SiO_2-ZnO-$CuPC$ layered structure as a sensor for NO_2. All experiments were performed with single delay-lines instead of a dual delay-line configuration. This was done because the reference delay-line also showed responses for various gases, e.g. an initial response of 44 Hz/ppm was observed for NO_2. In forthcoming experiments, the sensor would have to be coated with a passivation layer in order to prevent reference delay-line responses.

This present paper deals with the application of silicon nitride as a passivation layer on the sensor, yielding an Si-SiO_2-ZnO-nitride layered structure. The effect of passivation with the nitride was illustrated in two ways. Firstly, the effect on the response of the reference delay-line was measured. Secondly, a sensor coated with CuPC was studied as a gas sensor for NO_2. The CuPC was applied by physical vapour deposition (PVD) in two different ways: in between the two interdigital transducers and on the sensor as a whole.

5.2 Experimental part

The gases were obtained from Matheson: NO_2 (>99.5%), and HoekLoos: anhydrous NH_3 (>99.96%), N_2, O_2 and H_2 (all >99%). Water vapour was generated by evaporating pure liquid. The generated primary stream of vapours and gases was diluted with pressurized air (10% relative

humidity) which was purified over a charcoal bed. CuPC was obtained from Fluka A.G. and purified by vacuum sublimation at 0.05 mbar and 500 °C.

The starting material for the production of the silicon-based sensors was 1-10 Ohm.cm (100)[001] Si (300 μm thick) with a thermally grown SiO_2 layer (2 μm thick).

ZnO layers (about 20 μm thick) were fabricated by DC sputtering at 7 mTorr using 100% O_2 in a Varian 3119 R&D sputter station. The target-to-substrate distance was 9 cm and the substrate temperature 400 °C.

A 0.5 μm silicon nitride layer was applied by plasma-enhanced chemical vapour deposition starting from N_2, NH_3 and SiH_4 (330:3:1) at a rate of 26 nm/min at 1 Torr and 350 °C and an RF power density of 0.1 W/cm^2 at 100 kHz.

Evaporated CuPC layers were applied by physical vapour deposition at 10^{-5} Torr in a Balzers Union MED 010 system using an aluminium mask. The source-to-substrate distance was 8.5 cm, the source temperature was sufficient for a growth rate of 0.02 μm/min.

Table 7   Description of different sensor types: the frequency (f_0), drift (D) and peak-to-peak noise (N) at 150 °C as well as the "layer thickness" (d) of the CuPC layers

Sensor configuration[1]	Code	f_0 (MHz)	D (Hz/min)	N (Hz)	d (kHz)
Si-SiO$_2$-ZnO	CuPC135a	70	-5.6	90	-
Si-SiO$_2$-ZnO-PCPVD	CuPC134	70	-2.1	110	118
Si-SiO$_2$-ZnO-PCPVDA	CuPC135	70	-71.0	200	97
Si-SiO$_2$-ZnO-PCPVDA	PC153b	71	-8.5	110	107
Si-SiO$_2$-ZnO-nitride	SIN150	72	-0.2	20	-
Si-SiO$_2$-ZnO-nitride-PCPVDA	CPC154	72	-1.5	70	57
quartz	CuPC76a	80	-1.4	40	-
quartz-PCPVD	CuPC65	52	0.8	10	27
quartz-PCPVDA	CuPC76	80	-0.3	20	56

[1] PCPVD = CuPC layer applied in between IDTs,

PCPVDA = CuPC layer applied on sensor as a whole.

In Table 7 the different sensors studied are listed with their frequency, medium-term drift and peak-to-peak noise. The layer thickness can be expressed in terms of the sensor frequency shift due to the application of the layer. This value is included in Table 7.

A description of the experimental test system and definitions of response, response time and sensitivity have been previously published [30,31] or will be published in detail [46].

5.3 Results and Discussion

In Table 8, the sensitivities are shown for Si-SiO$_2$-ZnO-based sensors. For the sake of reference here, the sensitivities of the reference ZnO and quartz delay-lines are also given.

Table 8   Sensitivity normalized to 70 MHz of the different sensor types for NO$_2$, NH$_3$ and H$_2$O at 150 °C

Sensor configuration	Code	Freq. (MHz)	NO$_2$	NH$_3$ (Hz/ppm)	H$_2$O
Si-SiO$_2$-ZnO-PCPVD	CuPC134	70	200	-1.0	0.0
Si-SiO$_2$-ZnO-PCPVDA	CuPC135	70	920	-5.2	0.0
Si-SiO$_2$-ZnO	CuPC135a	70	40	-0.7	-0.1
quartz-PCPVD	CuPC65	52	36[1]	-2.9[1]	0.0
quartz-PCPVDA	CuPC76	80	-57[1]	2.8	0.0
quartz	CuPC76a	80	0	0.0[1]	0.0

[1] normalized to a 70 MHz base frequency (see text).

The sensitivity of a SAW sensor is related to the frequency of the device. This implies that the results given cannot be easily compared. In Table 8, calculated results are shown normalized to a frequency of 70 MHz using the theoretical relationship between the sensitivity and frequency squared.

It is observed that the sensitivity of the silicon-based sensor to NO$_2$ is larger than the quartz-based sensor even when compensated for differences in layer thickness and frequency. These results are in accordance with the work of Caliendo et al. [49]. They studied a palladium layer for the detection of hydrogen on Si-SiO$_2$-ZnO, quartz and lithium niobate and found comparable differences in response for the three types of sensors.

In Table 8, the results are listed for both CuPC in between the transducers and all over the sensor. Surprisingly, in the quartz system, application of a CuPC layer on the delay-line as a whole caused a change in the response sign as well as an increased absolute value, while in the case of the silicon-based sensor, the same configuration showed a higher response with the same sign.

The reference ZnO delay-line showed a response for NO_2, which is partly irreversible with an initial value of 40 Hz/ppm. A similar delay-line made out of quartz did not shown any response to NO_2. The ZnO reference delay-line also responded to water and ammonia.

As apparently bare ZnO is not able to play a satisfactory role as reference delay-line, in later experiments the ZnO was coated with a silicon nitride passivation layer in order to prevent the interaction between the ZnO and the analyte NO_2 or interferences. The passivated sensors showed less drift and noise when compared with the non-passivated silicon-based sensors (Table 7).

The SAW response mechanism is a combination of changes in mass, conductivity and elasticity and some other minor effects, as has already been postulated by several authors [24,53-56]. In this case, elasticity effects, like the other minor effects, are neglected because adsorption of a gas only slightly changes the elasticity coefficient of the materials involved: copper phthalocyanine, zinc oxide and silicon nitride.

The net mass change is due to adsorption of the analyte and/or the desorption of other compounds present at the surface (such as oxygen or water) which as a result can be positive or negative. If the mass change is a predominant factor, the resulting frequency response can be negative or positive. When both mass and conductivity changes determine the response, these effects work in the same or the opposite direction. In the case of an insulating silicon nitride layer on top of the semiconducting ZnO, the contribution to the SAW response of a changing conductivity resulting from the adsorption and/or desorption process may be neglected [58,59]. In this type of layered structure, the strength of the electric potential associated with the acoustic field decreases rapidly with the distance from the surface and may no longer play a role when the insulating layer is sufficiently thick. Venema et al. [58] are presently studying these phenomena in detail.

The effects of the presence of different gases on the *reference delay-lines* of both the non-passivated and the passivated sensors at 150 °C are shown in Table 9.

Table 9   Responses to various gases of the non-passivated (PC135a) and passivated (SIN150)
          reference delay-lines at 150 °C

Gas	Ref. gas	Conc. (ppm)	Response (Hz)	
			Non-passivated	Passivated
NO_2	air	44	1750	-30
NH_3	air	250	-180	-25
H_2O	air	12500	-1250	-300
O_2	air	400000	-480	-360
H_2	N_2	500000	-23000	-12500
air	N_2	-	-1450	-190

In general, the passivated sensors showed smaller responses to the different gases, especially in the
case of NO_2, suggesting that in the case of the non-passivated sensors, the conductivity and mass
changes work in the same direction with respect to the SAW response. Responses to other gases were
small, and high concentrations had to be applied to observe any response at all. With these gases,
the differences between non-passivated and passivated sensors were less pronounced than in the case
of NO_2, but significant improvements were observed. In the case of H_2O and O_2 in air and H_2 in
nitrogen, the disappointing effect of passivation may be caused by the diffusion of the gases through
the silicon nitride layer into the ZnO layer.

With respect to the *measuring delay-lines*, the sensitivity at 150 °C of both passivated and non-
passivated delay-lines is shown in Table 10. Upon passivation, a decreased sensitivity to NO_2 was
observed. Again this suggests that in the case of the non-passivated sensors, the conductivity and
mass changes work in the same direction with respect to the SAW response.

Table 10   Response at 150 °C to 50 ppm of NO_2 of a delay-line passivated with silicon nitride
           and non-passivated delay-line

Sensor Configuration	Code	Response to 50 ppm NO_2 (Hz)
Si-SiO_2-ZnO-PCPVDA	PC153b	6200
Si-SiO_2-ZnO-nitride-PCPVDA	CPC154	400

The relative responses (expressed as Hz/ppm divided by Hz/100 ppm NO_2 times 100) of the different sensors to ammonia and water are listed in Table 11. Again, very high concentrations had to be applied in order to obtain reliable results, especially in the case of water. Passivation caused higher relative responses to ammonia and water. As a result, non-passivated delay-lines at 150 °C seem to be favourable with respect to selectivity.

Table 11   Relative response (RR) at 150 °C to NH_3 (at 250 ppm) and H_2O (at 12,500 ppm) of different sensor configurations

Sensor configuration	Code	RR (NO_2 = 100)	
		NH_3	H_2O
quartz-PCPVDA	CuPC65	-5	0
Si-SiO$_2$-ZnO-PCPVDA	PC153b	-4	-0.02
Si-SiO$_2$-ZnO-nitride-PCPVDA	CPC154	-9	-0.13

5.4   Conclusions

Research on surface acoustic wave chemical sensors deals with the development of suitable chemical interfaces that transduce signals from the chemical domain to the physical domain as selectively as possible.

Preliminary results show the feasibility of a silicon-based SAW sensor system with an Si-SiO$_2$-ZnO-layered structure as a chemical sensor. The sensitivity of an NO_2 sensor of this type employing copper phthalocyanine as the chemical interface is higher than that of a similar system based on piezo-electric quartz.

Dual delay-line measurements with the silicon-based sensors to improve temperature stability and other common mode effects could only be performed when a passivation layer was applied, as bare ZnO interacts with all kinds of gases to give considerable responses from the *reference delay-lines*. For that purpose a silicon nitride layer was applied.

Application of the insulating silicon nitride layers caused different SAW responses on the reference delay-line not only as a result of the passivating effect, but also because the conductivity part of the SAW response mechanism may play a smaller role, yielding mass charges as the predominant effect. Upon passivation on the *measuring delay-line*, the sensitivity to NO_2 decreases which may also be caused by the different SAW response mechanism. Selectivity was also badly affected by passivation.

A good compromise between the positive effects on the reference delay-line and the negative effects on the measuring delay-line may be the following configuration: an Si-SiO$_2$-ZnO SAW sensor with a

passivated reference delay-line and a non-passivated measuring delay-line completely covered with the chemical interface. In this way the chemical interface itself acts as a "passivation layer". Work is in progress to study this compromise.

6 A SAW GAS SENSOR FOR CARBON DIOXIDE AND WATER. PRELIMINARY EXPERIMENTS.

6.1 Introduction

Surface Acoustic Wave (SAW) devices are attractive for chemical microsensor applications because of their small size, low cost, high sensitivity and good reliability. Furthermore, SAW technology is compatible with planar integrated circuit technology.

The first gas sensor using SAW was reported by Wohltjen et al. [31,60]. For the adequate measurement of a specific gas in a mixture of gases the delay-line of the SAW device must be coated with an appropriate chemical interface. The interactions occurring at the interface together with the basic structure behaviour are responsible for the performance characteristics of the gas sensor such as selectivity, sensitivity, reversibility and response time [29].

Much interest exists nowadays for a carbon dioxide (CO_2) gas sensor. There is in fact a need for an alternative for the infrared CO_2 detectors, which are currently in use, as these systems are large, expensive and require much maintenance.

Especially two main fields of application are in view: a CO_2 sensor to be applied in biotechnology, i.e. in fermentors for process control purposes, and a CO_2 sensor for biomedical applications to monitor the exhaled breath during surgical treatment and intensive care. For both categories a concentration range up to 10% vol. is required. In biotechnological applications, the sensor should be insensitive to oxygen, ammonia, organic acids and alcohol, whereas in a biomedical application the sensor should be insensitive to oxygen, nitrogen, water, nitrous oxide and other anaesthetic gases.

In order to develop a SAW gas sensor for CO_2, the search for a chemical interface which shows a selective and reversible interaction with CO_2 is of prime importance. In cases like this, one has to learn from the literature about interactions between CO_2 and chemical compounds. As a start, irreversible interactions have to also be included because sometimes irreversibility can be overcome by applying higher temperatures or temperature cycles.

The literature search revealed that all kinds of amines and imines, as well as zeolites, are used for a selective interaction with CO_2. Zeolites are crystalline inorganic compounds showing networks of SiO_4 and AlO_4 groups with different metal ions as counter ion. These compounds are often used in

CO_2 gas adsorption. However, the main problem with these compounds is their adhesion to the sensor surface. Therefore our prime interest was to apply amines or imines as the chemical interface. This article describes some preliminary experiments with poly(ethyleneimine): PEI.

6.2   Experimental part

The configuration of the quartz-based SAW devices and dual delay-line oscillator electronics to obtain a stable frequency signal is described in [25]. The experimental test system and definitions of response, response time and sensitivity are described in [30,31].

The PEI solution was applied on the SAW device as a dried drop or by an airbrush technique. With the dried drop method a small drop of the solution was put on the wave path of one delay-line and the solvent, in this case water, was allowed to evaporate. With airbrushing, a fine mist of the solution was sprayed on the surface of the sensor. In an attempt to produce a uniform coating on various sensors, the following method was applied: A solution of 1% by weight of PEI was sprayed with a Devilbiss Aerograph Sprite Major using nitrogen at 1 bar as propellant. The aerograph was mounted perpendicularly to the sensor surface in such a way that the distance between spray-nozzle and surface was 15 cm. One delay-line was covered with a mask (made out of paper) and the coating was applied on the other delay-line (both on the transducers and the wave path in between). The SAW frequency shift was monitored on a frequency counter while the temperature was kept at 70 °C. Several bursts of the spray resulted in a coating which produced a frequency shift of approximately -8000 Hz on a 40 MHz sensor, from which an average thickness of 37 nm was calculated, assuming a density of 1 g/cm^3 and a homogeneous coverage.

By spray-coating in the way described above, the thickness of the films are not equal, resulting in different responses. Practically, the responses of the various sensors may be compared dividing by the mass of the coating calculated from the frequency shift. In this calculation a linear relation between frequency change and mass change is assumed [13,60] although the limited validity of this assumption was learned from former experiments [30].

The poly(ethyleneimine) used in these studies was obtained from Hicol (Polymin P) as a 50% solution in water. From pH measurements, a dissociation constant pK_b of 3.41 was calculated.

6.3   Results and discussion

Response to CO_2: In the initial experiments, the response of a 40 MHz sensor to CO_2 was observed at different temperatures. The delay-line with about 1 μg of PEI showed an increase of the frequency signal upon exposure to 10% (volume per volume) of CO_2 in pressurized air with a relative humidity (RH) of 10%. At 30 °C no response was found; at 50 °C a slow positive response was

found which was larger at 70 °C, whereas at 90 °C again no response was observed. When going from 90 °C back to 70 °C and lower, the response to CO_2 had disappeared illustrating the destructive effect of heat or CO_2 on the response. It was also found that successive samplings at 70 °C caused the response to decrease illustrating CO_2 itself to be responsible for this insensitivity. Response times were about 4 min, whereas recovery times could not be determined due to the baseline drift occurring after exposure to CO_2. Therefore in Figure 6 only the initial responses of freshly prepared 40 MHz sensors with about 1 µg of PEI to a number of different CO_2 concentrations are depicted. The figure clearly illustrates that PEI shows an interesting interaction with CO_2.
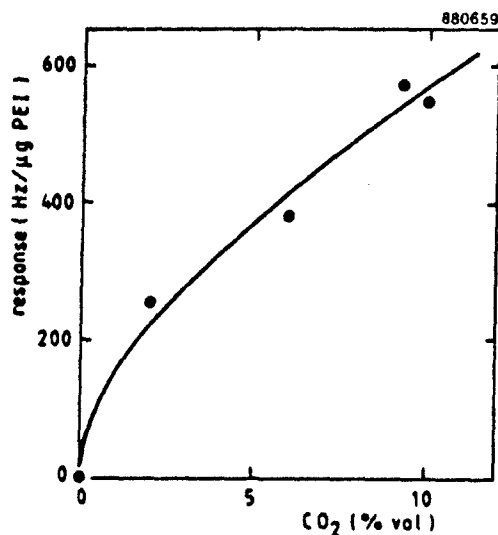

Figure 6   The initial response of different sensors with freshly prepared PEI layers to varying CO_2 concentrations at 70 °C
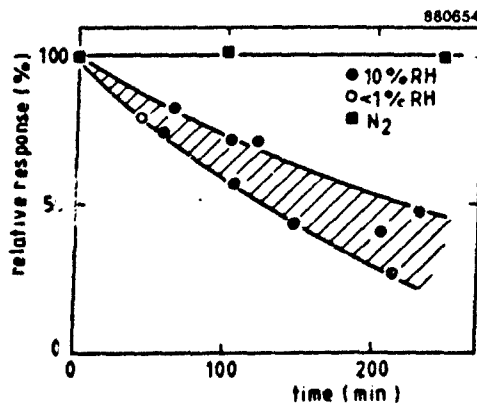
Figure 7   Relative decrease of sensitivity towards CO_2 with time in air and in a nitrogen atmosphere at 70 °C

Effect of oxygen on the response to CO_2: In Figure 7, the relative decrease of the CO_2 sensitivity with time is represented for most of the PEI sensors tested. In this figure the decrease of the sensitivity towards CO_2 in an N_2 atmosphere is also given. It can be seen that there are no great differences in the fatiguing rate of the various PEI sensors, except for the sensor measured in an N_2 atmosphere.

It was found that when the sensor was tested in air after being tested in an N_2 atmosphere a fast decrease in sensitivity towards CO_2 occurred immediately. The baseline drift increased when the purge gas was changed from N_2 to air. This could be explained by a certain loss of the PEI mass, although also a possible change in conductivity may play a role [29,60].

The conclusion from these results is that oxygen is responsible for the fatiguing processes of the PEI sensor's sensitivity to CO_2.
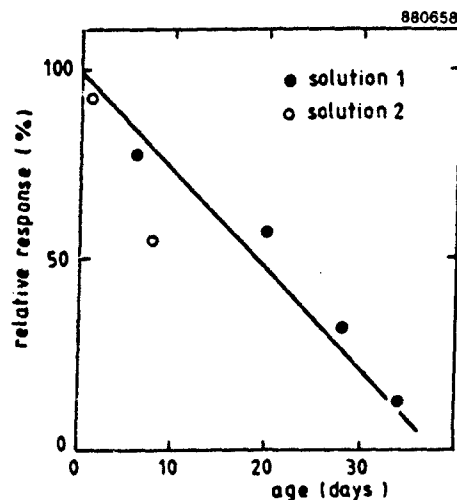
Figure 8   Relative decrease of sensitivity towards CO_2 at 70 °C in time during storage of two PEI solutions

Effect of the pH of the PEI solution on the sensitivity towards CO_2: It was noticed that coatings successively obtained from a stock solution containing PEI gave rise to a decreasing initial sensitivity towards CO_2. This effect is shown in Figure 8. Two solutions, prepared in the same way, were stored in glass flasks at room temperature. It is concluded that the solutions have to be freshly prepared just before applying them to the sensor.

Because the interaction between PEI and CO_2 is assumed to be an acid-base interaction as is illustrated in Figure 9, the pH of the solution might affect the sensitivity towards CO_2 of the PEI sensor prepared from this solution.

PEI solutions of different pH values, obtained by adding 2 M NaOH or 100% acetic acid, were used to prepare different PEI sensors. These were tested on their sensitivity with the results given in Table 12.
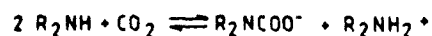
$$2\ R_2NH + CO_2 \rightleftharpoons R_2NCOO^- + R_2NH_2^+$$

Figure 9   Scheme describing the interaction between PEI and CO_2

Table 12   Response to CO_2 at 70 °C and 10% RH for sensors obtained by applying PEI solutions with different pH

pH PEI solution	Response (Hz/µg PEI)
5.0	10
7.9	230
10.8	555
12.0	325
13.0	20

Results show that every pH change of the PEI solution from the initial pH value of 10.8 has a negative effect on the sensitivity towards CO_2. The effect of the pH on the possible degradation of the PEI interface cannot be explained at the moment because of the lack of data.
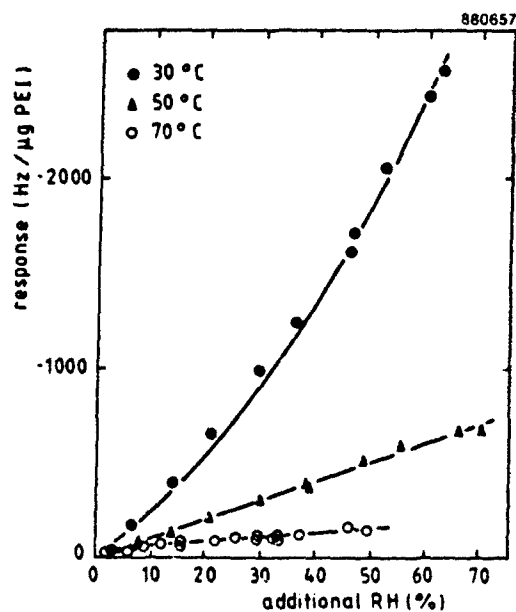

Figure 10   The response to 10% CO_2 of a 40 MHz sensor with PEI at 30, 50 and 70 °C as a function of relative humidity

Effect of water on the response to CO_2: Because of the assumed acid-base interaction of CO_2 with PEI, CO_2 responses were affected by the presence of H_2O. In order to understand this kind of interaction, measurements of the CO_2 sensitivity were also carried out in dry air (<1% RH). Surprisingly, here a negative initial response to 10% of CO_2 was observed: -830 Hz per µg PEI compared to +550 Hz per µg PEI at 10% RH. This indicates a different interaction at the chemical interface or a different response mechanism. Afterwards, the response to CO_2 was measured in air with 10% RH resulting in a positive response again.
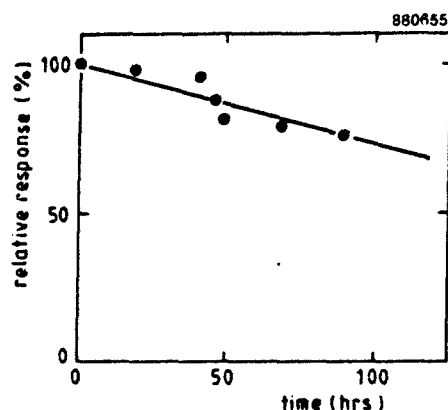

Figure 11   Relative decrease of H_2O sensitivity with time in air at 50 °C

Figure 10 shows the response to H_2O (in air containing ambient CO_2) of a 40 MHz sensor with 1.35 µg PEI at 30, 50 and 70 °C using a reference air flow containing 10% RH. It was found that the response time was around 1 min and that water has little influence on the baseline drift.

Figure 11 shows the relative decrease of the sensitivity towards H_2O versus time, at 50 °C. From this figure, a half-life time of about 200 hours can be derived compared to a half-life time of about 100 minutes for the CO_2 response at 70 °C.

Interferences: In Table 13 the results obtained so far are summarized showing the interferences from H_2O and O_2 on the response to CO_2, which make the sensor less suitable for CO_2. On the other hand, the high sensitivity observed for H_2O makes the system more suitable for a relative humidity rather than a CO_2 sensor. These considerations add to the research work on SAW sensors for relative humidity published so far [62-66] in which polymers have also been used as chemical interface applied both on quartz and on lithium niobate.

Table 13   Summary of the results obtained with the PEI sensors

Gas	RH (%)	Temperature (°C)	Sensitivity (Hz/µg.%)
CO_2	10	30	0
CO_2	10	50	7[1]
CO_2	10	70	55
CO_2	10	90	0
CO_2	<1	70	-83
CO_2[2]	10	70	-22
H_2O	-	30	-1420
H_2O	-	50	-395
H_2O	-	70	-220
EtOH	10	50	0
NH_3	10	50	-235[3]

[1] response time 15 min.

[2] in nitrogen atmosphere.

[3] measured in the 0-0.1% range.

In the table the interferences of both ethanol and ammonia are also presented. The NH_3 response is measured at only 0.1%. As generally the response curves tend to become less steep at higher concentrations, the interference in the same concentration range as water or CO_2 is less dramatic.

6.4   Conclusions

Upon applying poly(amines) as a chemical interface indeed a response for CO_2 was observed. However, degradation phenomena which are, up to now, not well understood occur when applying poly(ethyleneimine) as chemical interface. The degradation phenomena as well as the strong interference from water vapour renders the sensor not encouraging at the moment for CO_2 but might lead to the development of a SAW sensor for relative humidity. It depends on the application of such an RH sensor whether CO_2 will interfere.

Much work on the development of a SAW sensor for CO_2 needs to be done in order to obtain a sensor for application in biotechnology and biomedical technology. From this point, two pathways seem possible: one in which other polymers containing amines can be tried in order to obtain more stable responses towards CO_2 and less interference from water and other chemical species. Another

pathway would employ crystalline aluminosilicates (zeolites) as potential chemical interfaces. One of the most important problems is the applicability of the crystallites to the surface of the SAW device with reliability and reproducibility.

7 AN AUTOMATED SYSTEM FOR TESTING SURFACE ACOUSTIC WAVE GAS SENSORS

7.1 Introduction

In chemical sensors, chemical signals are transduced into the appropriate electrical signals. In contrast to physical signals there is always a variety of chemical signals present. As a consequence, selectivity is very important. If one uses a (bio)chemical interface, these requirements can often be met. The interface interacts with the analyte as selectively as possible, thereby modulating the flow of physical or electrical signals in the sensor device.

Surface Acoustic Wave (SAW) devices are attractive for chemical sensor applications because of their small size, low cost, sensitivity and reliability [10,12]. In these devices, acoustic wave phenomena occurring at the (bio)chemical interface are influenced by the presence of an analyte. SAW sensor technology as a whole has the potential of being applied on a surface rather than in a three-dimensional space. As a result, this technique is very compatible with planar silicon technology, thereby opening possibilities for applying both the sensor and the electronics on a single silicon-based device: a so-called smart sensor chip.

At our laboratory (bio)chemical interfaces are developed, applied to the SAW sensor surface in several ways and tested. When (bio)chemical interfaces are to be selected and in a next stage completely tested for selectivity, response time, reversibility, reproducibility, reliability, ageing and shelf-life, an extensive testing programme has to be performed.

In a number of papers [23-26,30,31,41,42,45] we have already reported on our SAW chemical sensor research concentrating on the development of a SAW gas sensor for NO_2. Metallo phthalocyanines were applied as the chemical interface.

In this paper, we describe our SAW testing system including an automated gas or vapour generation system (simply called gas generation system) and data acquisition system.

In the literature [67-73] many papers deal with the generation of test atmospheres for testing all kinds of systems including chemical sensors. Especially Grate et al. [72] describe a testing system for SAW chemical sensors. Our approach is significantly different. In building the system, we especially aimed at a highly efficient way of testing by utilizing the time after office hours by unmanned operation, even when testing the sensor with highly toxic compounds. As in one of our

research programmes to develop a SAW gas sensor for chemical warfare agents to be used as a warning or monitoring device by the military forces, special attention was paid to safety.

7.2 System description

General: To test many different (bio)chemical interfaces applied to SAW sensor devices, a variety of vapours and gases have to be generated in a large range of concentrations. Often the sensors must be characterized at different operating temperatures or relative humidities. A universal gas generation system was designed to dilute gases or to generate vapours from liquid compounds.

The efficiency of testing sensors at different parameters was improved by both controlling all the functions of the gas generation system and the sensor system, as well as data acquisition of the sensor output and other relevant parameters, by a computer.

These features make unattended operation possible by programming the testing parameters such as the operating temperature of the sensor, the duration of the test, the analyte concentrations, the time of exposure of the sensor, and the relative humidity.

System design: The material from which the gas generation system had been built up was chosen to be a combination of glass and stainless steel. Glass is attractive because of its inertness as some of the analytes are very corrosive compounds. Moreover the low adsorption properties of glass, its transparency (some kinds of contamination of the system can easily be observed) and its relatively low costs are of interest. Stainless steel tubing was used in those parts of the system which have to resist increased pressure. Connections between glass and stainless steel were made by means of Teflon ferrules adapted to standard Swagelock fittings.

Mass Flow Controllers (MFCs) were used for the accurate measurement and control of gas flows. Independent from the supply pressure and the temperature, these instruments pass through a fixed mass of gas adjustable by the electronic setpoint of the controller. An MFC consists of a flow sensor and an integrated control valve. The flow sensor contains a capillary tube provided with two temperature sensors. The difference in temperature sensed by the two sensors depends on the heat transfer properties of the gas flow. The heat transfer is determined by the mass of the gas flow and the specific heat and density of the gas. The difference between the output signal of the flow sensor and the setpoint signal is used to control the valve. The setpoint signal is determined by a potentiometer on the MFC central control unit, incorporating a digital read-out module, or by a remote setpoint from a computer. When using a gas with a specific heat and/or density different from air, the output reading must be corrected with the conversion factor stated by the manufacturer. For proper operation, the MFC requires a pressure difference of 0.2-0.5 bar between the supply and back pressure to force the gas into the capillary tube. The MFCs used in our laboratory are calibrated by a qualified institute every two years under standard conditions on air.

Generation of vapours from liquid compounds at room temperature can be done by using bubblers, permeation tubes or evaporators. Vapours of very volatile liquids are generated by using membranes, capillary tubes or at low temperatures using a cryostat. In our system an evaporator is used in most cases, see Figure 12.
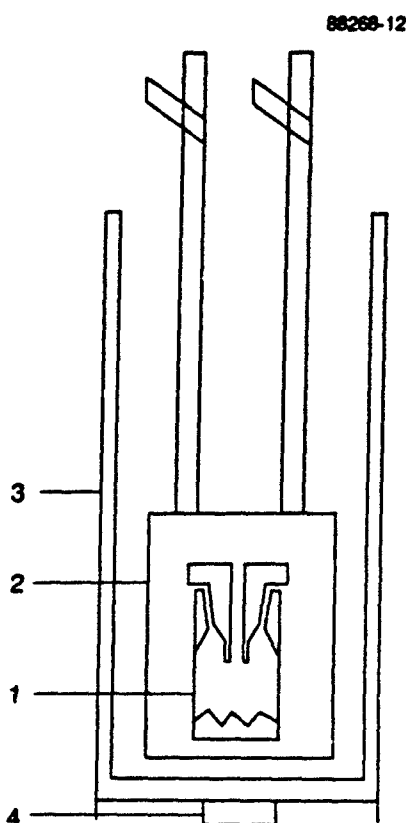
88268-12

Figure 12   Vapour generator. The numbers refer to the text

A small glass bottle (1) containing the liquid to be evaporated is placed in an evaporation vessel made of glass (2) provided with Teflon taps. This vessel is placed in a stainless steel heating jacket (3) supplied with a heating coil. The temperature is controlled by a Eurotherm 810 heating unit in combination with a NiCr/NiAl thermocouple. A safety switch (4) prevents temperatures exceeding 90 °C.
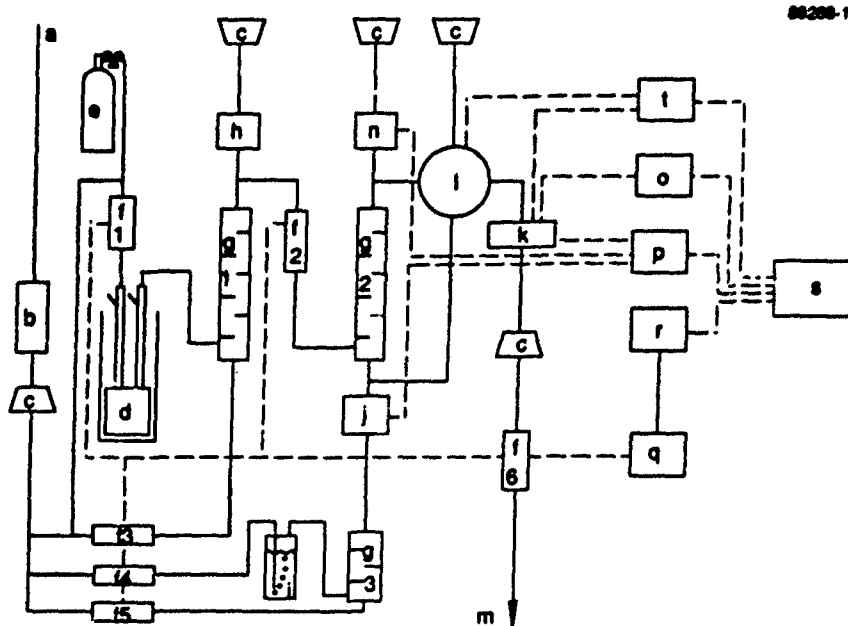
88288-13

Figure 13   Schematic representation of the complete experimental system. The solid lines
represent the tubing, while the dotted lines represent the data and control lines. The
numbers/letters refer to the text

In Figure 13 a schematic representation of the complete experimental system is depicted. Pressurized
air or another gas flow (a) is cleaned by an ultra-fine particle filter (Atlas Copco PD 7) (b) and a
charcoal filter (c). This flow is used as the carrier and the dilution gas. For monitoring the supply
pressure, a pressure gauge is mounted. From the vapour generator (d and Figure 12) or a gas bottle
(e), a primary gas flow, controlled by a Hi-Tec F201-EA MFC (f1) is diluted in a mixing vessel
(g1) with the gas flow from another MFC (f3). A part of the resulting gas flow is forced into the
second mixing vessel (g2) controlled by MFC (f2). To force this gas flow and to obtain the pressure
difference over this MFC (f2), required for correct operation, the pressure in the first dilution stage
is increased and controlled by a back pressure regulator (Veriflo BPR30) (h) and monitored by a
pressure gauge. In the second dilution stage, the gas flow from MFC (f2) is diluted with a second
diluting gas flow. This gas flow is a mixture of dry carrier gas controlled by MFC (f4) and a gas
flow containing water vapour from a bubbler (i), controlled by MFC (f5). Both gas flows are
previously mixed in mixing vessel (g3). The relative humidity is controlled by the ratio of
MFC (f4) and MFC (f5) and measured by a capacitive relative humidity meter (Novasina
TR-9) (j). If single stage dilution is needed, the evaporator (d) is connected directly to the second

mixing vessel (g2). From the resulting gas flow from vessel (g2), a gas flow of 10 L/h is drawn into the SAW measuring cell (k) via a six port pneumatically controlled stainless steel valve (Valco Instruments Co. Inc.) (l) upon the start of a measurement. This flow is controlled by MFC (f6), whose required pressure difference is obtained by a vacuum system (m). The final gas flow is monitored by a specific gas concentration monitor (n). Two types of monitors are used. Depending on the type of gas, an infrared monitor (Foxboro MIRAN 1A CVF) at an appropriate wavelength or a flame photometric phosphorus/sulphur detector (Meloy Labs Inc.) is used. The monitors are calibrated in a number of ways. In the case of generating vapours, the mass decrease of the liquid source in a certain period of time is used to calculate gas concentrations. In the case of diluting pure gases, the calibrated gas flows from the MFCs are used to calculate the gas concentrations. In some cases the gas or vapour is sampled by way of entrapment into impingers and analyzed by GC-analysis.

Waste gas flows are blown into the fume hood after being filtered by charcoal (c).

The SAW measuring cell, a milled brass box, contains the sensor device bonded to a ceramic substrate. The back of the substrate is provided with a thick film resistor for heating the sensor. The temperature of the sensor is measured by a temperature sensor (Analog Devices; two-terminal IC temperature transducer AD590L-F). The temperature sensor as well as the SAW device are fed by a 12 V DC power supply.

The SAW output frequency signals are measured with a frequency counter (Hewlett-Packard HP 5335A) (o). The analogue signals from the temperature sensor, the gas concentration monitor, the relative humidity meter and other signals are fed into a multiplexer and measured by a multimeter (HP 3478A) which serves as a multiple A/D converter (p). The MFCs are operated by the MFC central control unit (q). Remote setpoints for this control unit are generated by the central computer system (HP 86 B) (s) using D/A converters (r). The computer system is equipped with a disc drive unit (HP 9121) and a plotter (HP 7470A). High power D/A converters (t) are used as a programmable power supply for heating the sensor and switching the control valve to activate the pneumatically controlled valve (l).

The data acquisition system collects the number of the measurement, the frequency signals of both delay-lines of the SAW sensor, the dual delay-line signal being equal to the difference between both frequencies, the signal from the temperature sensor, the signal from the gas concentration monitor and the point of time of the measurement. These signals are stored on a floppy disc in blocks of 30 measurements, preventing loss of data by failures of the electricity or the computer system. Stored data can be retrieved for presentation on screen or plotter for further analysis.

Software: The software for performing the SAW sensor measurements and controlling the instrumentation and gas generation system was developed using the HP-BASIC language peculiar to HP 85/86 computers. Part of the software concerns the regulation of the generated gas concentrations. The calibration curves of the gas concentration monitors are mathematically fitted into an equation and integrated into the software. The output signal from the gas concentration monitor is converted to a concentration value using those calibration curves and is compared with the desired concentration. A proportional integral differential (PID) regulator calculates the new concentration output. Upon this concentration output the setpoints of the MFCs are calculated based on a minimum stochastic error in the resulting concentration. In this way a feedback of the concentration signal is realized. Similar regulating systems are present for thermostating the sensor device in the range 20-150°C and controlling the relative humidity in the range from 10-100%.

Accuracy and precision of the gas generation system: The accuracy of the MFCs used amounts to 1% full scale. As a result, most stable concentrations are obtained using all MFCs at setpoints as high as possible to reach the desired concentrations. The noise of the output signal of the gas concentration monitor is a measure for the accuracy of the concentration. The precision of the concentration is determined by the calibration procedure. Accuracy and precision of the generated concentrations depend largely on the type of gas or vapour.

Safety measures: As many compounds are used which are harmful to the environment, especially to human health, the complete gas generation system is placed in a continuously ventilated fume hood. The ventilation system is provided with two safety measures. Firstly, a flow sensor verifies the operation of the ventilation system. Secondly, a gas monitor system is placed into the fume hood close to the gas generation system. When ventilation stops or when the alarm level of the gas monitor is exceeded, an alarm system is activated, which in turn switches off the complete experimental system. By this action the generation is stopped, so the exhaust of gas from the system is minimized.

7.3 Evaluation and performance of the gas generation system

Concentration range: Because of the possibility of choosing one- or two-stage dilution, a large range of concentrations can be reached. When diluting a pure gas the concentration range is 0.5-200,000 ppm, assuming 5% of the maximum capacity of a MFC to be the minimum setpoint. Vapours can be generated at lower concentrations depending on the physical properties of the compound.

Temperature stability: The feedback control of the temperature of a SAW sensor device described above results in the rapid heating of the device with very little overshoot and a very stable temperature within ± 0.02 °C of the desired temperature. Figure 14a shows the heating of a sensor up to 150 °C taking 10 minutes and the change of the frequency signal of the sensor. Figure 14b is a magnification of a part of Figure 14a, showing the stability of the temperature of the sensor and the frequency signal.
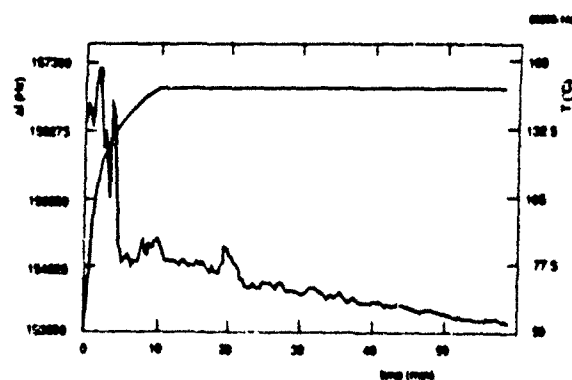

Figure 14a   The temperature and frequency signal of a SAW device at heating up to 150 °C
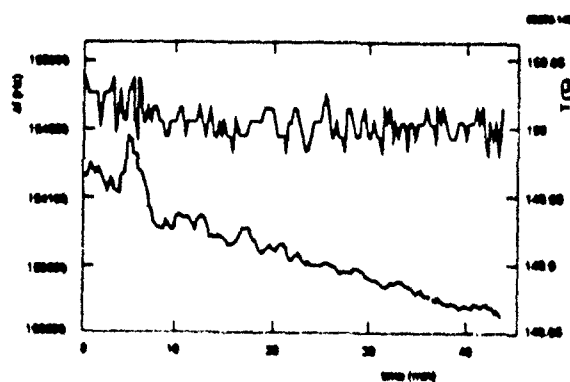

Figure 14b   Magnification of a part of Figure 14a showing the stability of temperature and frequency output

Response rates: The overall response time of the sensor is defined as the time from opening the sample valve until the establishment of a stable sensor signal. This overall response time is

composed of the time needed for the sample gas to reach the sensor, i.e. the dead time, the time needed to reach a homogeneous concentration inside the measuring cell and the response time of the sensor itself. The latter consists of the time needed for the gas molecules to diffuse (in)to the active sites of the chemical interface of the sensor, the time needed for interaction of the gas with the chemical interface, ranging from adsorption to chemisorption, and the time needed for transduction of the chemical signal via a physical signal into an electrical signal.

The dead time and the time needed to reach a homogeneous concentration are determined by the dead volume of the system from the sample valve to the sensor as well as by the flow rate of the sample gas to the sensor. The dead volume, including the measuring cell, amounts to 16.5 cm^3. At a flow rate of 10 L/h in our system it takes 6 seconds to fill the measuring cell with the sampled gas. An homogeneous concentration is assumed after flushing the cell seven times taking 42 seconds. However, the first sensor response can be induced by the first gas molecule reaching the sensor taking only 0.15 seconds, as the tubing between valve and cell is 24 cm in length and 0.15 cm in internal diameter.

The flow rate of 10 L/h is chosen from experiments with a variable value using a fast responding sensor, i.e. our most rapidly responding sensor obtained until now. So, the response time of the sensor does not completely determine the overall response time, not masking the dead time and time to reach a homogeneous concentration.

The above-mentioned experiments were performed with a 52 MHz SAW device applied with poly(ethyleneimine) at the chemical interface. This sensor was exposed to water vapour with a relative humidity of 50% with regard to 7% of the reference air flow.
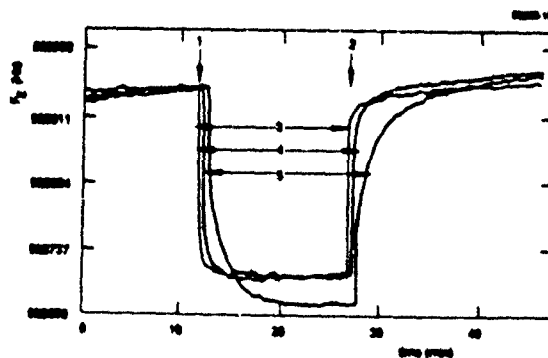

Figure 15   Responses of a SAW sensor to water vapour at three different gas flow rates. (1). sampling on. (2). sampling off. (3). flow rate 0.6 L/h. (4). flow rate 2.0 L/h. (5) flow rate 13.0 L/h.

Figure 15 shows the sensor response at three different flow rates of the sample gas, 0.6, 2.0 and 13.0 L/h, respectively . When the flow rate was reduced, the overall response time increased, caused by an increase of the dead time, the time needed to reach a homogeneous concentration and possibly the diffusion time. At the slow flow rate of 0.6 L/h, the response increased as well, indicating another equilibrium state between the gas and the chemical interface. Possibly, the equilibrium has been shifted by a change in the pressure caused by the changing flow rate.
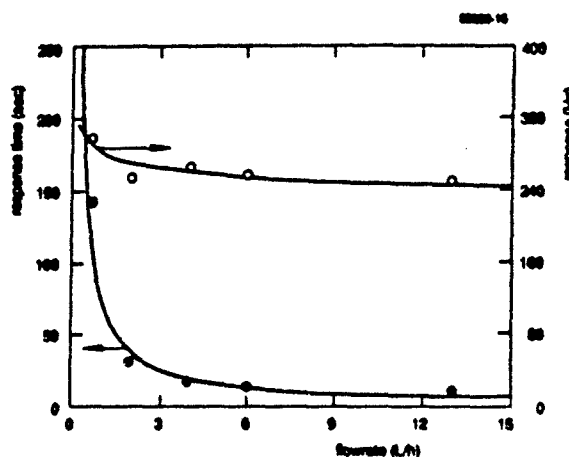

Figure 16   The influence of the flow rate of the gas on the overall response time and the SAW
sensor response

Figure 16 represents the influence of the flow rate on the overall response time and the response. At flow rates above 6 L/h, the overall response time and the response are independent of the flow rate. In a number of cases, Guilbault et al. [74-77], the flow rate also affects the response of acoustic sensors. AT-cut crystals (bulk acoustic wave devices) were used with different coatings. When methyltrioctylphosphonium dimethylphosphate was used as a coating the response to phosgene decreased upon an increasing flow rate. This effect was explained by the weak adsorption of phosgene, causing easy desorption from the substrate at high flow rates [74]. When mononitrotoluenes were detected with a coating of Carbowax 1000, a maximum response was found at a flow rate of 1.8 L/h. This observation was explained as follows. Above this flow rate the adsorption is incomplete, while below this flow rate the diffusion of the analyte causes the lower response [75]. A similar maximum was observed in the detection of acetoin using semicarbazide as a coating. The maximum appeared at 6 L/h in dry nitrogen and at 12 L/h in air with a relative humidity of 58% [76]. When using tetrakis(hydroxy-ethyl)ethylenediamine as a coating for CO_2 the response decreased below a flow rate of 3.6 L/h and was nearly constant above this value [77]. All

explanations suggested by Guilbault et al. raise questions. Further studies have to be performed in order to obtain a good view on the effect of flow rates on the SAW sensor response. For instance, a lower pressure at higher flow rates may affect the adsorption (and therefore the response) which is not isobaric any longer.

Output: An example of the output of the experimental system is given by Figure 17, showing the result of more than 20 hours unattended operation. A SAW sensor applied with a layer of copper phthalocyanine as the chemical interface was exposed seven times to different concentrations of NO_2 ranging from 50 to 300 ppm at an operating temperature of 150°C. The concentration of NO_2 was measured by the infrared monitor and stored on a floppy disc. The concentration signal and the frequency signal of the sensor are combined in one plot.
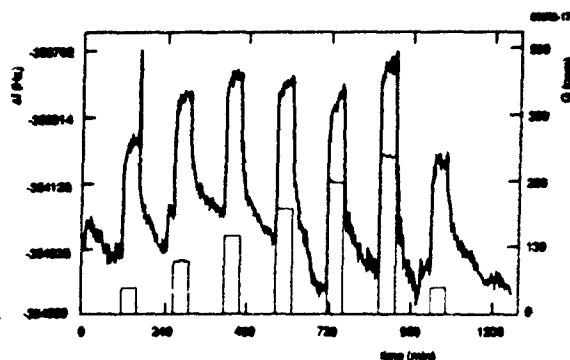

Figure 17   Output of the experimental system after exposing a SAW sensor to different concentrations of NO_2 at an operating temperature of 150 °C

From such a plot, a response versus concentration graph is made, accounting for the drift and the not yet reached equilibrium. Figure 18 represents the relation of the sensor response with the gas concentration deduced from Figure 17.
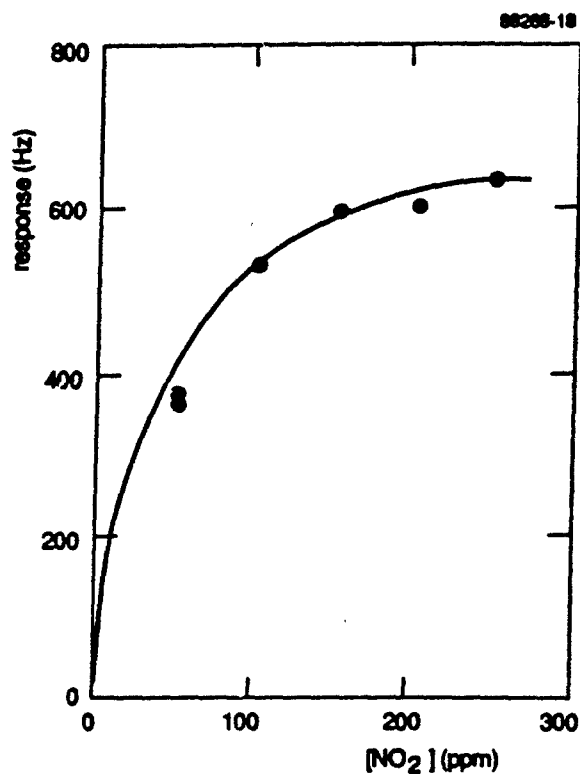
Figure 18   Response versus concentration curve deduced from Figure 17

7.4   Conclusions

In our laboratory, an automated, reliable, and safe system for testing SAW gas sensors has been developed. The system includes the possibility to generate and/or dilute almost any gas or vapour and can easily be adapted for testing sensors or equipment other than SAW sensors.

A highly efficient way of testing has been realized by unattended operation in a safe way. A large range of concentrations is achievable by the option of single stage or two-stage dilution.

The reliability of the gas generation system is guaranteed by the continuous monitoring of the concentration of the gas generated by using Mass Flow Controllers. Both monitors and Mass Flow Controllers are periodically calibrated.

A-specific sampling effects on the sensor response are excluded by using the same flow for dilution and reference gas flow.

One of the limitations of the system is the fixed concentration range during one test after one has chosen single stage or two-stage dilution. Another restriction at the moment is that only one type of gas or vapour can be generated during one test. This can easily be overcome by extending the system in the future. Moreover, the possibility exists to change the system to enable the generation of mixtures of gases/vapours along with the simultaneous testing of more than one sensor device.

A future development will be the modification of the measuring cell and the sampling system in order to reduce the dead volume. This will be important for testing fast responding sensors (response time below one minute).

8   CONCLUSIONS

This third progress report deals with the on-going work at the Prins Maurits Laboratory TNO on Surface Acoustic Wave (SAW) chemical sensors. This report is in addition to the four reports dealing with the work on the development of a SAW sensor for chemical warfare agents [37-40]. Achievements in the field of acoustics and the developments of new device configurations, studies on existing chemical interfaces and the development of new chemical interfaces, as well as the development of an experimental test system, are presented in the different chapters which all have appeared or will appear in the scientific literature.

Immobilization of chemical interfaces. It was clearly observed in the case of an immobilized copper phthalocyanine derivative used as a chemical interface for NO_2, that response times, recovery times and sensitivity of such a sensor are smaller due to the much thinner interface layer. For several applications, response times are still too long mainly resulting from polymerization of the spacer molecule. It is to be expected that true monolayers will further improve response times as well as selectivity. Therefore extensive studies to obtain monolayers, using other spacers and/or reaction conditions are in progress, together with the application of higher sensor frequencies and with the help of advanced surface analysis tools.

Silicon-based SAW sensors. Preliminary results showed the feasibility of a silicon-based SAW sensor system with a $ZnO-SiO_2-Si$-layered sensor configuration. The sensitivity of an NO_2 sensor of this type using copper phthalocyanine as the chemical interface was much higher than the quartz-based system. Dual delay-line measurements with the silicon-based sensors to improve temperature stability and other common mode effects could only be performed when a silicon nitride passivation layer was applied, as bare ZnO interacts with all kinds of gases to give considerable responses of the reference delay-lines. Experiments proved the passivating effect on the reference delay-line. Upon passivation the sensitivity to NO_2 of the measuring delay-line decreased and selectivity was badly
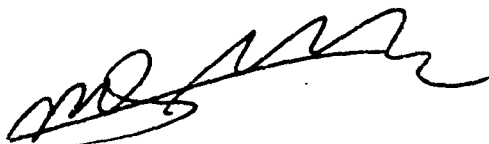
affected as well. A good compromise between the positive effects on the reference delay-line and the negative effects on the measuring delay-line may be the following configuration: an $Si-SiO_2-ZnO$ SAW sensor with a passivated reference delay-line and a non-passivated measuring delay-line completely covered with the chemical interface. In this way the chemical interface itself acts as a "passivation layer". Work is in progress to study this compromise.

SAW sensor for CO_2. Upon applying poly(ethyleneimine) as a chemical interface, a response for CO_2 was indeed observed. However, degradation phenomena occurred which are not well understood up to now. These degradation phenomena as well as the strong interference from water vapour renders the sensor not encouraging at the moment for CO_2 but might lead to the development of a SAW sensor to measure the relative humidity.

Much work on the development of an alternative chemical interface needs to be done. Other polymers containing amines may be tried in order to obtain more stable responses towards CO_2 and less interference from water. Another pathway would employ crystalline aluminosilicates (zeolites).

Automated SAW sensor test system. In our laboratory, an automated, reliable, and safe system for testing SAW gas sensors has been developed. The system includes the possibility to generate and/or dilute almost any gas or vapour and can easily be adapted for testing sensors or equipment other than SAW sensors. A highly efficient way of testing has been realized by unattended operation in a safe way. A large range of concentrations is achievable by the option of single stage or two-stage dilution.

9   AUTHENTICATION

M.S. Nieuwenhuizen

(Project leader/author)

10   REFERENCES

1. Nylander, C.; J. Phys. E: Sci. Instrum. 1985, 18, 736

2. Janata, J.; Bezegh, A.; Anal. Chem. 1987, 60, 62R

3. Janata, J.; Anal. Chem. 1990, 63, 65

4. Edmonds, T.E.; "Voltammetric and Amperometric Transducers" in Chemical Sensors,
    ed. Edmonds, T.E.; Blackie, Glasgow, 1987, 193

5. Edmonds, T.E.; "Potentiometric Transducers in Chemical Sensors" in Chemical Sensors,
    ed. Edmonds T.E.; Blackie, Glasgow, 1987, 214

6. Janata, J.; "Chemically Sensitive Fieldeffect Transistors in Solid State Chemical Sensors"
    ed. Janata, J.; Huber, R.J.; Academic Press, Orlando, 1985, 66

7. Williams, D.E.; "Conduction and Gas Response of Semiconductor Gas Sensors" in Solid
    State Gas Sensors, ed. Moseley, P.T.; Tofield, B.C.; Adam Hilger; Bristol, 1987, 71

8. Culshaw, B.; Proc. 4th Int. Conf. on Sensors and Actuators, Tokyo, 1987, 462

9. Harmer, A.L.; Narayanaswany, R.; "Spectroscopic and Fibre-optic Transducers" in Chemical
    Sensors, ed. Edmonds, T.E.; Blackie, Glasgow, 1987, 275

10. Nieuwenhuizen, M.S.; Venema, A.; Sensors and Materials 1989, 5, 261

11. Nieuwenhuizen, M.S.; Venema, A.; "Mass sensitive devices" in Chemical Sensors, ed. Goepel, W.; Lundstrom, I.; Verlag Chemie, Weinheim, 1991, pp. 648-680

12. Fox, C.G.; Alder, J.F.; The Analyst, 1989, 114, 997

13. Wohltjen, H.; Dessy, R.; Anal. Chem. 1979, 51, 1458

14. Wohltjen, H.; Dessy, R.; Anal. Chem. 1979, 51, 1465

15. Wohltjen, H.; Dessy, R.; Anal. Chem. 1979, 51, 1470

16. Wohltjen, H.; US Patent 4312328 (1979)

17. Vetelino, J.F.; Lee, D.L.; WO appl 8301511 (1983)

18. Bryant, D.L.; Lee, D.L.; Vetelino, J.F.; Proc. IEEE Ultrasonics Symp., Chicago, 1981, 171

19. D'Amico, A.; Palma, A.; Verona, E.; Sensors and Actuators 1982, 3, 31

20. Martin, S.J.; Schwartz, S.S.; Gunshor, R.L.; Pierret, R.F.; J. Appl. Phys. 1983, 54, 561

21. Martin, S.J.; Schweizer, K.S.; Schwartz, K.S.; Gunshor, R.L.; Proc. IEEE Ultrasonics Symp., Dallas, 1984, 207

22. Martin, S.J.; Schweizer, K.S.; Ricco, A.J.; Zipperian, K.E.; Proc. 3rd Int. Conf. on Sensors and Actuators, Philadelphia, 1985, 71

23. Barendsz, A.W.; Vis, J.C.; Nieuwenhuizen, M.S.; Vellekoop, M.J.; Ghijsen, W.J.; Venema, A.; Proc. IEEE Ultrasonics Symp., San Francisco, 1985, 586

24. Nieuwenhuizen, M.S.; Barendsz, A.W.; Nieuwkoop, E.; Vellekoop, M.J. and Venema, A.; Electronics Letters 1986, 22, 184

25. Venema, A.; Nieuwkoop, E.; Vellekoop, M.J.; Barendsz, A.W.; Nieuwenhuizen, M.S.; Sensors and Actuators 1986, 10, 47

26. Venema, A.; Nieuwkoop, E.; Vellekoop, M.J.; Ghijsen, W.J.; Barendsz, A.W.; Nieuwenhuizen, M.S.; IEEE Trans. on Ultrasonics, Ferroelectrics and Frequency Control 1987, 34, 148

27. Venema, A.; Vellekoop, M.J.; Nieuwkoop, E.; Haartsen, J.C.; Nieuwenhuizen, M.S.; Nederlof, A.J.; Barendsz, A.W.; Proc. 4rd Int. Conf. on Sensors and Actuators, Tokyo, 1987, 481

28. Vellekoop, M.J.; Nieuwkoop, E.; Haartsen, J.C.; Venema, A.; Proc. IEEE Ultrasonics Symp., Denver, 1987, 641

29. Nieuwenhuizen, M.S.; Barendsz, A.W.; Sensors and Actuators 1987, 11, 45

30. Nieuwenhuizen, M.S.; Nederlof, A.J.; Barendsz, A.W.; Anal. Chem. 1988, 60, 230

31. Nieuwenhuizen, M.S.; Nederlof, A.J.; Anal. Chem. 1988, 60, 237

32. Barendsz, A.W.; Nieuwenhuizen, M.S.; Proc. Int. Symp. Protection Against Chemical Warfare, Stockholm, 1986, 165

33. Nieuwenhuizen, M.S.; Barendsz, A.W.; Int. J. of Environm. Anal. Chem. 1987, 29, 105

34. Barendsz, A.W.; Nieuwenhuizen, M.S.; Dutch Patent 8502705 (1985), European Patent 239609 (1987) and WO appl. 8702135 (1987)

35. Barendsz, A.W.; Nieuwenhuizen, M.S.; "SAW chemosensor. First progress report", Report PML-TNO 1986-6

36. Nieuwenhuizen, M.S.; Jong, L.P.A. de; "SAW chemosensor. Second progress report", Report PML-TNO 1987-24

37. Jong, L.P.A. de; "Experiments aiming at the development of a SAW biochemical sensor for nerve agent detection", Report PML 1990-61

38. Nieuwenhuizen, M.S.; Nederlof, A.J.; "SAW sensor for chemical warfare agents 1. General introduction and preliminary results with the chemical interfaces FPOL and PEM. ", Report PML-TNO 1991-85

39. Nederlof, A.J.; Nieuwenhuizen, M.S.; "SAW sensor for chemical warfare agents. 2 Evaluation of some lanthanide coordination compounds as chemical interfaces using the nerve agent simulant DMMP", Report PML-TNO 1992

40. Nederlof, A.J.; Nieuwenhuizen, M.S.; "SAW sensor for chemical warfare agents. 3 Continued evaluation of some lanthanide coordination compounds as chemical interfaces using the nerve agent GB", Report PML-TNO 1992

41. Nieuwenhuizen, M.S.; Nederlof, A.J.; Coomans, A.; Fres. Z. Anal. Chem. 1988, 330, 123

42. Nieuwenhuizen, M.S.; Nederlof, A.J.; Vellekoop, M.J.; Venema, A.; Sensors and Actuators 1989, 19, 385

43. Nieuwenhuizen, M.S.; Nederlof, A.J.; Vellekoop, M.J.; Venema, A.; Proc. Int. Meeting on Chemical Sensors, Cleveland, 1990

44. Nieuwenhuizen, M.S.; Nederlof, A.J.; Sensors and Actuators B, to be published

45. Nieuwenhuizen, M.S.; Nederlof, A.J.; Sensors and Actuators 1990, B2, 97

46. Nieuwenhuizen, M.S.; Nederlof, A.J.; Rev. Sci. Instrum., to be published

47. Shirai, H.; Yagi, S.; Suzuki, S.; Hojo, N.; Makromol. Chemie 1978, 178, 1889

48. Shirai, H.; Maruyama, A.; Kobayashi, K.; Hojo, N.; Urishido, K.; Makromol Chemie 1980, 181, 581

49. Caliendo, C.; D'Amico, A.; Verardi, P.; Verona, E.; Proc. IEEE Ultrasonics Symp., Chicago, 1988, 334.

50. Vellekoop, M.J.; Visser, C.C.G.; Proc. IEEE Ultrasonics Symp., Chicago, 1988, 265

51. Visser, J.H.; Vellekoop, M.J.; Venema, A.; Drift, E. van der; Rek, P.J.M.; Nederlof, A.J.; Nieuwenhuizen, M.S.; Proc. IEEE Ultrasonics Symposium, Montreal, 1989, 195

52. Chuang, C.T.; White, R.M.; Bernstein, J.J.; IEEE Electron device Letters 1982, 3, 145

53. Venam, A.; Humphries, R.F.; IEEE Electronics Letters 1977, 13, 594

54. Ricco, A.J.; Martin, S.S.; Zipperian, T.E.; Sensors and Actuators 1985, 8, 319

55. Snow, A.W.; Barger, W.R.; Klusty, M.; Wohltjen, H.; Jarvis, N.L.; Langmuir, 1986, 2, 513

56. White, R.M.; Proc. 41st Annual Frequency Control Symp., 1987, 333

57. Lee, R.; Vetelino, J.F.; Falconer, R.S.; Xu, Z.; Proc. IEEE Ultrasonics Symp., Chicago, USA, 1988, 585

58. Venema, A.; Vellekoop, M.J.; personal communication

59. Venema, A.; "Transduction and propagation of surface acoustic waves in three-layered media with an electrically conducting substrate", Thesis Delft, The Netherlands

60. Wohltjen, H.; Sensors and Actuators, 1984, 5, 307

61. Martin, S.J.; Frye, G.C.; Ricco, A.J.; Zipperian, T.E.; Proc. IEEE Ultrasonics Symposium, Denver, USA, 1987, 563

62. Brace, J.G.; Sanfelippo, T.S.; Proc. 4th Int. Conf. on Sensors and Actuators, Tokyo, Japan, 1987, 467

63. Brace, J.G.; Sanfelippo, T.S.; Joshi, S.G.; Sensors and Actuators, 1988, 14, 47

64. Joshi, S.G.; Brace, J.G.; Proc. Int. Symposium on Moisture and Humidity, 1985, 225

65. Joshi, S.G.; Proc. IEEE Ultrasonics Symposium, San Francisco, USA, 1985, 600

66. Huang, P.H.; Proc. 4th Int. Conference on Sensors and Actuators, Tokyo, Japan, 1987, 462

67. "Controlled test atmospheres. Principles and techniques", ed. Nelson, G.O.; Ann Arbor Sci. Publ., Michigan, 1971

68. Barratt, R.S.; The Analyst 1981, 106, 817

69. Namiesnik, J.; J. Chrom. 1984, 300, 79

70. Woodfin, W.J.; Am. Ind. Hyg. Assoc. J. 1984, 45, 138

71. Weber, H.; Stenner, H.; Kettrup, A.; Fres. Z. Anal. Chem. 1986, 325, 64

72. Grate, J.W.; Ballantine, D.S.; Wohltjen, H.; Sensors and Actuators 1987, 11, 173

73. Harvey, I.; Coles, G.; Watson, J.; Sensors and Actuators 1989, 16, 393

74. Suleiman, A.A.; Guilbault, G.G.; Anal. Chim. Acta 1984, 162, 97

75. Tomita, Y.; Ho, M.H.; Guilbault, G.G.; Anal. Chem. 1979, 51, 1475

76. Hahn, E.C.; Suleiman, A.A.; Guilbault, G.G.; Anal. Chim. Acta 1987, 197, 195

77. Fatibello-Filho, O.; Andrade, J.F. de; Suleiman, A.A.; Guilbault, G.G.; Anal. Chem. 1989, 61, 746

1. Hoofddirecteur DO-TNO

2. D.W.O.O.

3. HWO-KL

4/5. HWO-KLu

6. HWO-KM

7. Hoofd Afdeling Militair Geneeskundig Beleid
   Directoraat Generaal Personeel
   Ministerie van Defensie

8. Coördinator Grootschalige Rampenbestrijding
   Ministerie van Binnenlandse Zaken
   Drs. H. Evers

9. Adviseur van het Prins Maurits Laboratorium TNO
   Prof. Dr. J.M. van Rossum

10. Adviseur van het Prins Maurits Laboratorium TNO
    Chemische Research
    Prof.Dr. G. Dijkstra

11. HBur. NBC
    Ir. A.A.M. Slagveer

12. Lid van de Contact Commissie NBC-Bescherming
    Ir. M. Vertregt
    Afd. Wetenschappelijk Onderzoek KL

13. Lid van de Contact Commissie NBC-Bescherming
    Lkol.arts S. Schroten
    Plv. Hfd. Afd. AMZ van de IGD KL

14. Lid van de Contact Commissie NBC-Bescherming
    KLTZ R.A. Baljeu
    Hfd. van de School voor NBCD en Bedrijfsveiligheid

15. Lid van de Contact Commissie NBC-Bescherming
    DMKL/HWZ/MILIEU/NBC
    Dr. T. Deinum

16. Lid van de Contact Commisie NBC-Bescherming
    Lkol. R. Peeters
    Commandant NBC-school KL

17. Lid van de Contact Commissie NBC-Bescherming
    Drs. N.H.W. van Xanten
    Beleidsmedewerker Militair Toxicologie
    Afd. Militair Geneeskundig Beleid

18. Lid van de Contact Commissie NBC-Bescherming
    Ir. LTZT1 M. Hendriks
    Marstaf/TAKT/NBCD

19. Lid van de Contact Commissie NBC-Bescherming
    Lt.Kol. J. Koopmans
    Staf CLaS/BLS
    Ffd. Afd. Operatiën, Bureau NBC

20. Lid van de Contact Commissie NBC-Bescherming
    Maj. W. Doppenberg
    Afd. Operationele Behoefte van de Luchtmachtstaf
    Sectie GWGRO-1

21. Lid van de Contact Commissie NBC-Bescherming
    Maj.dierenarts H.W. Poen
    Beleidsmedewerker Wetenschappelijk Onderzoek
    Afd. Militair Geneeskundig Beleid

22. Lid van de Contact Commissie NBC-Bescherming
    Ir. Th. Sijbranda
    Hfd. Sectie Klinische Chemie en Toxicologie IGD KL

23. Lid van de Contact Commissie NBC-Bescherming
    Mw. A.C. Grade, arts
    Directie Militair Geneeskundige Diensten

24. Lid van de Contact Commissie NBC-Bescherming
    Stafapotheker IGD KLu
    Kap.-apotheker E. Lam

25. Lid van de Contact Commissie NBC-Bescherming
    KLTZT K. Brijder
    PFS/TECHN-W/HNBCD

26. Lid van de Contact Commissie NBC-Bescherming
    A.S. de Koning, arts
    Hfd. Bureau Wetenschappelijk Onderzoek DMGB

27. Inspectie Geneeskundige Dienst KLu
    Hoofd Afdeling Operationele Geneeskunde

28. Inspecteur Geneeskundige Dienst (KL)

29. Inspecteur Geneeskundige Dienst (KLu)

30. Inspecteur Geneeskundige Dienst (Zeemacht)

31/33. Hoofd van het Wetenschappelijk en Technisch
       Documentatie- en Informatiecentrum voor de Krijgsmacht

34. Lid Instituuts Advies Raad PML
    Prof. Dr. G. Blasse

35. Lid Instituuts Advies Raad PML
    Prof. dr. U.A.Th. Brinkman

36. Directeur van het Medisch Biologisch Laboratorium TNO
    Prof.Dr. W.R.F. Notten

37. Directeur van het Prins Maurits Laboratorium TNO
    Ir. E.B. van Erp Taalman Kip

38. Directeur Technologische Research van het Prins Maurits Laboratorium TNO
    Dr.Ir. H.J. Pasman

39. Directeur Chemische Research van het Prins Maurits Laboratorium TNO
    Ir. M. van Zelm

40. Archief Prins Maurits Laboratorium TNO

41. Documentatie Prins Maurits Laboratorium TNO

42/43. Reserve-exemplaren

44/45. H.L. Boter

46/47. M.S. Nieuwenhuizen

48. dr R. Scott (CBDE, UK)

49. dr O. Busmundrud (NDRE, Noorwegen)

december 1991

REPORT DOCUMENTATION PAGE
(MOD NL)

1. DEFENSE REPORT NUMBER (MOD-NL) TD91-4194	2. RECIPIENT'S ACCESSION NUMBER	3. PERFORMING ORGANIZATION REPORT NUMBER PML1992-88
4. PROJECT/TASK/WORKUNIT NO. 118488268	5. CONTRACT NUMBER A88/K/416	6. REPORT DATE February 1992
7. NUMBER OF PAGES 52 0 annexes	8. NUMBER OF REFERENCES 77	9. TYPE OF REPORT AND DATES COVERED Final

10. TITLE AND SUBTITLE

SAW chemosensor. Third progress report.
(SAW chemosensor. De derde voortgangsrapportage.)

11. AUTHOR(S)

M.S. Nieuwenhuizen

12. PERFORMING ORGANIZATION NAME(S) AND ADDRESS(ES)

TNO Prins Maurits Laboratory
P.O. Box 45, 2280AA Rijswijk, The Netherlands

13. SPONSORING AGENCY NAME(S) AND ADDRESS(ES)

DMKL
P.O. Box 90701, 2509 LS The Hague

14. SUPPLEMENTARY NOTES

15. ABSTRACT (MAXIMUM 200 WORDS (1044 BYTE))

At the Prins Maurits Laboratory TNO, work on surface acoustic wave (SAW) chemical sensors is being performed. Up to now the main subjects have been: implementation of SAW technology on a silicon chip, the development of a SAW sensor for NO_2 and the development of a SAW sensor for chemical warfare agents. This third progress report deals with the on-going work on a SAW sensor for NO_2 including immobilization of the chemical interface, silicon-based SAW sensors for NO_2 with and without the application of silicon nitride passivation layers, preliminary results of the development of a SAW sensor for CO_2 and a chapter dealing with an automated SAW testing system developed at TNO-PML. Most of the chapters have been published in the literature.

16. DESCRIPTORS	IDENTIFIERS	
Nitrogen Dioxide Silicon Silicon Nitride Carbon Dioxide Tests	Chemical Detectors Surface Waves Acoustics Chemical Agent Detection Immobilization	Chemical Interface

17A. SECURITY CLASSIFICATION (OF REPORT) UNCLASSIFIED	17B. SECURITY CLASSIFICATION (OF PAGE) UNCLASSIFIED	17C. SECURITY CLASSIFICATION (OF ABSTRACT) UNCLASSIFIED
18. DISTRIBUTION AVAILABILITY STATEMENT Unlimited distribution		17D. SECURITY CLASSIFICATION (OF TITLES) UNCLASSIFIED